Impact of guaiacol on the formation of undesired macromolecules during catalytic hydroconversion of bio-oil: a model compounds study

Matthieu Ozagac, Céline Bertino-Ghera, Denis Uzio, Mickael Rivallan, Dorothée Laurenti, Christophe Geantet

Impact of guaiacol on the formation of undesired macromolecules during catalytic hydroconversion of bio-oil: a model compounds study

M. Ozagac[a], C. Bertino-Ghera[a,*], D.Uzio[a], M. Rivallan[a], D. Laurenti[b], C. Geantet[b]

[a]*IFP Energies Nouvelles, Rond-point de l'échangeur de Solaize, BP3, 69360 Solaize, France*

[b]*IRCELYON, UMR5256 CNRS-UCBL, 2 avenue A. Einstein, 69626 Villeurbanne cedex, France*

**Corresponding author: celine.bertino-ghera@ifpen.fr*

Abstract

Although catalytic hydroconversion of pyrolysis bio-oils has been studied for many years, side reactions such as condensation or oligomerization leading to high molecular weight compounds still need comprehensive studies. In this work, the catalytic hydroconversion of D-glucose, furfural, acetic acid and guaiacol representative of pyrolysis bio-oils was investigated separately before testing a 5-component mixture. Thanks to a detailed analytical strategy (i.e. SEC, ^{13}C NMR, GC, HPLC), this paper focuses on the effect of guaiacol conversion on sugar-like macromolecules. The study of single D-glucose and furfural revealed the fast production of high molecular weight compounds (up to 700 g.mol^{-1}) that were proven to further precipitate (from D-glucose). Guaiacol addition led to a decrease of the solid production through solubilizing and/or reacting with macromolecules. This phenomenon produced larger soluble macromolecules (up to 5.000 g.mol^{-1}). Results show that guaiacol and its hydroconversion products formed soluble macromolecules at short reaction times and low temperatures.

Keywords: biofuels; macromolecules characterization; pyrolysis bio-oil; guaiacol; D-glucose; SEC

1. Introduction

Lignocellulosic biomass is a promising feedstock that could be used as a renewable and CO_2-neutral source of energy and is expected to be an important resource for liquid transportation fuels or chemicals in a near future. Lignocellulose is commonly composed of three major fractions: 40–45 wt% of cellulose (dry composition), 25–35 wt% of hemicelluloses, 15–30 wt% of lignin and up to 10 wt% of other compounds (such as minerals) [1]. The most widely studied softwood feedstock are pine (or spruce), and cork or oak as regard to hardwoods. Flash pyrolysis is a thermochemical process used to transform these resources into liquid [1, 2]. However, the obtained pyrolysis bio-oils have limited end-user application due to their acidity (Total Acid Number or TAN between 70 and 120), their low heat capacity (compared to fossil fuels), their immiscibility with hydrocarbons and their thermal instability resulting from high oxygen content [3]. Oxygen is present in organic compounds but also as free water which can represent up to 30 wt% of the raw bio-oil. Since the last three decades, many laboratories have tried to perform

deoxygenation process inspired from petroleum feedstock catalytic hydroconversion [4]. However, upgrading biomass-derived oils from flash pyrolysis liquefaction to hydrocarbons requires a significant oxygen removal (and consequently a high H_2 consumption) before any final conventional refining process.

Also called upgrading, those thermo-chemical processes deal with operational temperatures up to 400°C. Nevertheless, several literature studies [4, 5] showed the occurrence of fast competitive reactions such as condensation or oligomerization which are prone to produce solid residues even at low temperature. This phenomenon is detrimental for the process because it leads to extensive plugging of the reactor and catalyst deactivation. This coking ability especially due to the bio-oils thermal instability is a process limitation and needs an in-depth comprehension before any industrial scaling-up. Venderbosch [5, 6] and Elliott [7] published studies describing the competition between hydroconversion pathways and the production of high molecular weight compounds also referred as soluble macromolecules [8 – 10]. To avoid those pathways, they recommended a two-step process to firstly convert macromolecules precursor at low temperatures (from 150 to 200°C) followed by a deep hydrodeoxygenation (up to 350°C). So far, the involved reaction mechanisms are not well described and literature is largely lacking of rationalization of the chemical mechanisms.

The pyrolytic degradation products of lignin were generally represented by aromatic model compounds [10 – 12] such as guaiacol, anisole or phenol derivatives. On the one hand, carbohydrates, acids, ketones and furans derivatives were commonly used to represent the contribution of cellulose and the hemicellulose [12, 13] fractions in the flash pyrolysis liquefaction. Levoglucosan [14, 15] and D-glucose [16] are typically adopted as representative compounds. Even if levoglucosan would be the model of choice as it is present in high quantity in pyrolysis bio-oils, it is readily converted to D-glucose in hydroconversion conditions and in acidic water medium [15 - 17]. On the other hand, it is well established [18, 19] that hemicelluloses flash pyrolysis produces furanic and carboxylic acid compounds in large amounts. Besides well identified molecules, heavier molecules including macromolecules are also present in the bio-oil (including pyrolytic lignin) and those macromolecules usually precipitated by water addition. These oligomers were characterized by typical aromatic fragments arising from lignin [10, 20]. Our purpose in this study is to investigate the macromolecules production from light molecules during the hydroconversion reaction.

Numerous studies deal with representative model molecules of bio-oils composition which result from lignocellulose [11] degradation during the pyrolysis step. Because of the high diversity of oxygenated compounds in a bio-oil, it is mandatory to consider at least a mixture of representative compounds even if very few studies were proposed in the literature. For a catalysts screening, Elliott [21] developed a three-compound mixture made of guaiacol, furfural, acetic acid and water. More than thirty by-products were

quantified but no crossed-interactions between those compounds were discussed. More recently, Runnebaum [22] has studied the catalytic conversion of four compounds representing a pyrolysed lignin fraction. Nevertheless, none of those experimental studies complied with the comprehension of the high molecular compounds production.

In this paper, we have chosen D-glucose as the ex-cellulose model molecule and arising compounds from hemicellulose flash pyrolysis were represented by furfural and acetic acid. In a previous work [23] we investigated the catalytic hydroconversion of D-glucose and furfural and we observed the fast and extensive production of high molecular weight compounds even at 200°C. This trend was followed by SEC analysis and carbon balances including GC-quantified compounds. Those so called macromolecules were proven to arise from furanic and aromatic compounds that were extensively produced by D-glucose dehydration and furfural hydrolysis/hydration. In the present work, we report the catalytic hydroconversion of a mixtures constituted by D-glucose, furfural and guaiacol. Through an increase of the complexity of the mixtures and using a multi-technique characterization strategy (SEC, ^{13}C NMR, GC, HPLC, etc…), this study highlights the main routes responsible for the formation of high molecular compounds and the effect of the presence of guaiacol on macromolecules.

2. Materials and Methods

2.1. Material

The D-glucose (> 99.5%), furfural (99%) and acetic acid (99%) were purchased from Sigma Aldrich and guaiacol (> 99%) from Acros Organics and n-hexadecane (99%) from Alfa Aesar. Those compounds were used as received.

To promote the hydroconversion reactions, various mono- and bi-metallic active phases were investigated. Noble metal based catalysts such as Pt, Pd or Ru exhibit high performances but remain expensive. Less performing Ni/alumina-based catalysts [24 - 26] are nevertheless an economically suitable solution for an industrial process. A proprietary NiMo/γ-Al_2O_3 catalyst (9.2 wt% Ni, 5.4 wt% Mo) displaying hydrothermal resistance was provided by Axens. Before each reaction, fresh catalyst was crushed and sieved to particle size from 1 to 2 mm and was reduced using a hydrogen flow (0.30 $m^3.h^{-1}$) at atmospheric pressure and 400°C during 2 h.

2.2. Experimental procedures

All catalytic reactions were carried out in an isothermal 500 cm^3 stainless steel autoclave equipped with an electromagnetic driven stirrer (Rushton impeller). The methodology used and the reproducibility of the experiments are described in Supplementary Fig. S1 and S2. For each run, 150 g of feed were introduced followed by 15 g of freshly reduced catalyst transferred in a basket in an argon vessel avoiding any post-oxidation. The

reactor was hermetically closed and purged by substituting air by nitrogen and finally by hydrogen. The initial pressure of hydrogen was set to 3.0 MPa before temperature increase.

The reaction temperature ranged from 200 to 300°C. In order to limit the catalytic reactions during the heating ramp (15 min to reach 250°C), the feed was vigorously stirred (1,200 RPM) only once the reaction temperature was reached. This procedure was adopted in order to limit the D-glucose conversion during the heating time. Stirring is maintained during cooling down. The hydrogen addition was set to maintain a constant total pressure of 13.0 MPa during the run. This procedure has been applied considering the maximization of the hydrogen consumption during the catalytic hydroconversion of an aqueous D-glucose (20 wt%) solution. Considering those stirring rates and catalyst beads size, no external hydrodynamic limitations have been observed [23].

Once the reaction time was reached, H_2 introduction was stopped and the reactor was cooled down to room temperature (10 min to cool down from 300 to 100°C). Then gaseous, liquid and solid products were totally collected and separately analyzed. Gases were collected using an auxiliary vessel and sampled in vacuum TEDLAR® bags for subsequent off-line gas chromatography (GC-FID/TCD) analysis. While the reactor was purged by nitrogen and unlocked, the catalytic basket was removed. The liquid phases and the solid residues were separated by centrifugation at 4,000 $tr.min^{-1}$ during 20 min. Subsequently, aqueous and organic phases were separated in a separatory funnel referred respectively as “aqueous phase” and “organic phase”. The recovered catalyst was washed using a Thermo Scientific™ Dionex™ (ASE 150) extractor heated at 60°C and under a 10 MPa acetone pressure. The catalyst and the solid residues were dried at 70°C under atmospheric pressure during 12 h. Acetone was used as a washing solvent also to clean the reactor and the impeller and was further removed by a vacuum rotary evaporator. The obtained liquid phase will be referred as “washed phase”.

2.3. Analytical procedures

Considering the complexity of the products, an analytical strategy was set to characterize each effluent (see Supplementary Fig. S3). Each phase was analyzed separately in order to determine the repartition of the carbon and to identify a maximum of compounds.

Gases were analyzed by GC (Agilent 7890A) equipped with a Flame Ionization Detector (FID) and two Thermal Conductivity Detectors (TCD). Three parallel columns were used: HP-Plot Q (30 m x 0.32 mm i.d x 20 µm), HP-Plot 5A (30 m x 0.32 mm i.d x 1 µm) and PONA (50 m x 0.2 mm i.d x 0.5 µm). The carrier gas was helium. Standards were periodically injected for alkanes (C1 to C6), CO, CO_2, N_2 and H_2 quantification. The oven temperature program ranged from 30 to 200°C at a rate of $20°C.min^{-1}$.

Liquid effluents were analyzed by GC (AGILENT-6890N) with a Flame Ionization Detector (FID) and a RTX-35 Amine (30 m x 0.25 mm i.d x 1 µm) column. The vaporization temperature was 250°C, the oven temperature program ranged from 40 to 220°C at a rate of 4°C.min^{-1}. For each identified compounds, quantification was performed with 1,2-propanediol as an external standard and Effective Carbon Number method (ECN) was used to estimate FID response factors for oxygenates [27]. The GC/MS analysis was conducted with a Thermo Trace GC/MS equipped with the same columns and program than the GC/FID analysis. The mass analyzer is a simple quadrupole with an electron ionization ion source at 70 eV. The products were identified using the NIST library.

The composition of the aqueous phase was also determined using a HPLC system (Waters Alliance 2695), a Bio-Rad column Aminex Deashing followed by an Agilent column Metacarb operated at 95°C. The aqueous mobile phase was set at a flow rate of 0.1 cm^3.min^{-1}. The detector is constituted of a Differential Index Refractometer and an UV detector. The analysis of a sample was complete within 100 min. The concentrations of each compound (cellobiose, D-glucose, sorbitol, xylose, galactose, arabinose, mannose, glycerol and xylitol) in the product mixture were determined using eight calibration curves obtained by analyzing standard solutions of known concentrations.

Water content in liquid effluents was measured by a Karl Fischer (KF) Mettler Toledo V20. For every sequence, a calibration procedure with a Fluka Hydranal water standard 1.0 was performed. Each value indicated in this study corresponds to average of three measurements.

Soluble macromolecules contained in aqueous effluents were analyzed by non-quantitative size exclusion chromatography (SEC) by a Waters system (Alliance). The system was constituted by four columns in series (7.8 mm × 300 mm) containing 5 µm-particle size with porosity ranging from 10 to 1,000 nm. During a typical analysis 50.10^{-6} m^3 of sample were injected into the column. Run were performed at 30°C (columns temperature) during 49 min. Two detectors were used: a refractive index-detector and a UV-detector (set to three wavelengths: 214, 254 and 280 nm). Tetrahydrofuran was used as mobile phase (1 cm^3.min^{-1}). Standard polystyrene mixtures having various molecular weights were used for calibration at the beginning of each new sequence and correspond to a Polystyrene (PS) molecular weight ranging from 160 to 5,000 g.mol^{-1}.

In order to determine the carbon balance, a Thermo Scientific™ FLASH 2000 analyzed the carbon deposition (CHONS) onto the catalyst and the solid residues. Grinded samples were injected twice in an oven set at 950°C where CO_2 was formed. An on-line TCD detector quantified this component and calculated the sample corresponding carbon equivalent. Each six samples, the analyzer was controlled by a BBOT (2,5-Bis (5-tert-butyl-benzoxazol-2-yl) thiophene) standard.

Finally, solid phase ^{13}C MAS NMR analysis were performed on an AVANCE Bruker 400 MHz with Highpower Proton Decoupling (HPDEC) and spinning rates of 12 kHz using a CPMAS probe and 4 mm rotor. The free induction decays were obtained after excitation with 90° pulses with a repetition time of 50 s. After accumulation of 1024 scans, spectra were processed with 20 Hz Lorentzian line broadening and a 0.1 s Gaussian broadening. All ^{13}C MAS NMR spectra were referenced to tetramethyl silane (TMS). Quantification of the functional groups present in each sample was determined after baseline correction by integrating over characteristic regions using TopSpin 3.0 software. Intensities over defined chemical shift windows were integrated to quantify selected C structures; 0-55 ppm (C-alkyl), 55-95 ppm (O-alkyl C including carbohydrates), 95-165 ppm (C-aromatic), 165-220 ppm (C-carbonyl in carboxylic acids, esters, amides, ketones and aldehydes).

2.4. Determination of the conversion, mass and carbon balances

As shown by the analytical strategy described previously, this study aims at understanding model compounds hydroconversion from the macroscopic scale (though experimental balance given by the Equation 1) to the molecular scale. In order to assess the accuracy of chemical pathways, carbon balances are considered taking into account each recovered phases as detailed in Equation 2. In the liquid phases, recovered carbon corresponds either to equivalent quantified carbon thought GC-FID and HPLC for the liquid phase or by Total Organic Carbon (TOC) and liquid elementary analysis (CHONS). When n-hexadecane has been used, elementary analysis of containing mixtures has not been considered.

Equation 1 : mass balance

$$\text{Experimental mass loss (expressed in weight \%)} = \frac{\left(m_{liquid}+m_{gases}+m_{catalyst}\right)_{introduced} - \left(m_{liquid}+m_{gases}+m_{catalyst}+m_{residues}\right)_{recovered}}{\left(m_{liquid}+m_{gases}+m_{catalyst}\right)_{introduced}} \times 100$$

Equation 2 : carbon balance

$$\text{Total quantified carbon (expressed in weight \% of carbon equivalent)} = \frac{\left(mC_{liquid}\right)_{introduced} - \left(mC_{liquid}+mC_{gases}+mC_{catalyst}+mC_{residues}\right)_{recovered}}{\left(mC_{liquid}\right)_{introduced}} \times 100$$

The gaseous phase is analyzed by GC-FID/TCD and the solid residues and the catalysts are assessed by a solid elementary analysis (CHNS).

Solving the Equation 2 implies considering the carbon contribution of each quantified species. Hence, carbon contribution of a molecule so called "A" constituted of carbon, oxygen and hydrogen atoms leads to:

Equation 3

$$mC_j = wt\%C_j . m_j \text{ and } mC_{liquid} = \sum_{i=j}^{k} mCi$$

With:

- mC_j: mass of carbon equivalent in the compound j [g].
- $wt\%C_j$: weight carbon content of the compound j [wt%].
- m_j: mass of GC-quantified compound j [g].
- $\sum_{i=j}^{k} mCi$: sum of the carbon equivalents hold by the compounds "j" to "k" in the liquid phase [g].

To consider the molecular scale, reactant (expressed as "A") conversion will be expressed as:

Equation 4

$$X_i = \frac{n_{A,0} - n_A}{n_{A,0}}$$

with :

- X_A : conversion rate of "A" reactant
- $n_{A,0}$ and n_A : "A" reactant molar amount respectively at the beginning and the end of the reaction [mol].

In order to compare SEC analyses with various water content liquid phases, raw signals will take into account the water dilution. Thus, signals will be presented as:

Equation 5 :

$$\text{Nomalized SEC signal} = \frac{Raw\ signal}{100mg} . \frac{1}{1 - Water\ content} = \frac{Raw\ signal}{100mg} . \frac{1}{Organic\ content}$$

With:

- Raw signal / 100: Raw signal (RI or UV) normalized to a 100 mg sample [mg^{-1}].
- Water content: weight water content in the liquid phase [-].
- Organic content: weight organic content in the liquid phase [-].

The carbon content of solids resulting from D-glucose hydroconversion during a test "i" containing n-hexadecane (noted as n-C16) onto the surface assessed by solid ^{13}C MAS NMR. Hexadecane was calibrated thanks to an external calibration (see supplementary Figure S4). Due to the intensity of hexadecane chemical shifts, the corresponding areas

were calculated and further subtracted to the ^{13}C NMR spectra. Thus, carbon equivalent in the solid residues were calculated following Equation 6.

Equation 6 : Carbon content in the D-glucose' residues "i" containing n-C16 assessed by solid ^{13}C MAS NMR :

$$m_{cor\,i} = m_{raw\,i} - m_{n-C16}$$

With:

- $m_{cor\,i}$: Corrected carbon equivalent mass of the residues for a test "i" [g].
- $m_{raw\,i}$: mass of carbon equivalent in the residues measured by elementary analysis for a test "i" [g].
- $m_{n\text{-}C16\,i}$: Carbon equivalent mass of n-hexadecane in solid residues quantified by external calibration of the ^{13}C MAS NMR [g].

2.5. Studied mixtures

As previously described, four model molecules have been chosen for this study: D-glucose (noted as Glu) in water, furfural (noted as Fur), acetic acid (noted as AA) and guaiacol (noted as Gua).

Mixtures (see Table 1) aimed at representing well known oxygenated functions compounds but also the proportions of related families of compounds as well as pH, C-H-O atomic ratios, water content in a typical raw bio-oil [1]. Thus, guaiacol was chosen to represents the pyrolyzed lignin fraction and was introduced either at 15 or 30 wt%. D-glucose and furfural modeling respectively carbohydrate-like and their degradation compounds were introduced at 20 and 13 wt% respectively. 30 wt% of demineralized water was introduced to model free water that is contained in a typical bio-oil but also to insure the D-glucose solubility in the liquid phase at ambient conditions. Finally, 7 wt% of acetic acid was introduced to set a representative bio-oil acidity with a Total Acid Number of 120 mg potassium hydroxide introduced for one gram of mixture.

In this work, the four-compounds mixtures will be noted as "Mixture A". A second mixture in which a part of guaiacol has been replaced by n-hexadecane will be noted as "mixture B". Those mixtures comply with average bio-oil atomic ratios (dry basis) [1]. "Mixture A" H/C and O/C atomic ratios are respectively equal to 1.4 and 0.6 whereas "Mixture B" H/C and O/C atomic ratios are respectively equal to 1.8 and 0.7.

The next section is divided into three parts.

- The first part will be focused on the catalytic hydroconversion from single compounds to the final mixture "A". For both single reactants and the ternary mixtures (e.g. three-compound mixtures) hydroconversion reactions, n-

hexadecane has been introduced in order to complete the feed loading to 150 g. For simplicity, the binary mixtures (e.g. two-compound mixtures) are reported in appendix. Whatever the studied mixture, 30 wt% of demineralized water was introduced. In this paragraph, chemical pathways will be discussed depending on hydroconverted mixtures.

- In a second and third part, the effect of reaction time and temperature on the Mixture A catalytic hydroconversion will be discussed. Those studies will particularly emphasize the effect of guaiacol (study of Mixture "B") on soluble macromolecules production.

3. Results and discussion

3.1. Study of the catalytic hydroconversion leading to "Mixture A"

In these experiments, the reaction time and temperature were respectively set to 1 h and 250°C. These conditions can be considered as usual ones regarding to bio-oil hydroconversion studies [4, 6 - 8].

Table 2 reports the experimental mass balances of the catalytic hydroconversion of eight mixtures from the single reactant to the ternary mixtures and Mixture A. Mass balances closures depend on the residue production which requires the use of a large quantity of acetone as a washing solvent further evaporated in a vacuum rotary evaporator. This last step has been identified as the main source of loss by evaporating lights compounds dragged by the acetone. When there is no solid residues production, mass balances are between 97.3 and 101.4 wt%, whereas when a large quantity of solids is produced, the mass balance is between 81.3 and 88.3 wt%.

In the case of the conversion of single molecules, only D-glucose led to residues in a large amount (8.0 g for 100 g of feed, representing 39 wt % with respect to the D-glucose loading). Considering Glu/Fur/AA mixture, the solid production increased up to 14.7 for 100 g of feed. Nevertheless, this content was drastically reduced when guaiacol was added to D-glucose and acetic acid in water (1.2 g for 100 g of feed). So, guaiacol had a remarkable effect on the solid production. In comparison with the Glu/Gua/Fur mixture, the catalytic hydroconversion of Mixture A also demonstrated that acetic acid promotes the solids production. Indeed, 11.2 g of solids residues were produced against 0.7 g from the Glu/Gua/Fur mixture.

To get an insight on soluble macromolecules properties, SEC-RI analyses of the aqueous and organic phases from the ternary mixtures and Mixture A are reported respectively in Figure 1 [A] and [B]. SEC-RI of hydroconverted single D-glucose and furfural effluents were described elsewhere [23].

When D-glucose was present in the feed, soluble components ranging between 200 and 400 g.mol^{-1} polystyrene equivalent (or PS eq.) were systematically observed in the aqueous phases (Figure 1 [A]). Moreover, considering the huge amount of solid residues produced during the catalytic hydroconversion of the ternary mixture D-glucose/furfural/acetic acid (see Table 2), it can be hypothesized that produced macromolecules were no more soluble in the aqueous phase and thus precipitated into the solid phase.

For ternary mixtures, this property was observed as long as guaiacol was not introduced in the feed. Then, the presence of guaiacol led to the formation of an organic phase. Corresponding SEC-RI analyses (Figure 1 [B]) indicate the production of heavy compounds up to 7,000 g.mol^{-1} PS eq.. This may suggest that macromolecules produced from the aqueous fraction (D-Glucose, Furfural) were no more precipitated into the solid phase but solubilized by the organic phase in presence of guaiacol. This interesting result will be further discussed. Without D-glucose (as shown by the Gua/Fur/AA test), it is also interesting to note that resulting components arising from furfural catalytic hydroconversion were mainly lower than 200 g.mol^{-1} PS eq. in the aqueous phase.

As it has been studied in our previous work [23], D-glucose single catalytic hydroconversion produces a wide range of chemicals since the chromatographic analysis of liquid phase enables the identification and quantification of 46 organic compounds. Main identified reactions were hydrogenolysis (production of levulinic acid or furfural), hydrogenation (production of sorbitol and alcohol compounds from ketones [28]), dehydration/hydration (production of 5-HMF or lactic acid) retro-aldol reaction (production of propane-1,2,3-triol, propane-1,2-diol [29] and acetic acid), decarboxylation or decarbonylation. Considering furfural single catalytic hydroconversion, we quantified 35 compounds involving furfural decarbonylation that produced C4 cut (furan and tetrahydrofuran) and furfural hydrogenation to C5 cut (furfuryl alcohol and by-products) [30 – 32]. In the same way, guaiacol catalytic hydroconversion in similar operating conditions involved the quantification of 20 compounds GC-FID analysis. It is commonly accepted [33, 34] that three main chemical pathways can be observed involving either the demethylation to 1,2-benzenediol or a direct demethoxylation step to phenol. The direct hydrogenation of the benzene ring is unfavored with NiMo/Alumina catalyst [35, 36]. Some studies [37, 38] also reported the production of heavier structures due to self-condensation between primary products such as catechol. Nevertheless, none of them has been clearly identified during this study.

Regarding the production of high molecular weight compounds reported by SEC-RI analyses (Figure 1), it appeared interesting to consider the carbon balances. Thus, a global carbon balance (Table 3) considering TOC and CHONS analysis respectively of the aqueous and organic phases was evaluated for the *Mixture A* catalytic hydroconversion effluents (experimental mass balance reported in Table 2). The initial introduced amount of carbon

is 58.9 g. Taking into account the experimental and the analytical errors, the carbon balance for this experiment is achieved by only 1.5 wt% loss. Mixture A catalytic hydroconversion led to a solid phase (as residue and coke onto the catalyst) which contains 25.3 wt% of the initial introduced carbon. The three liquid phases represent 71.3 wt% of C and the gaseous phase 2.0 wt% of C (particularly through CO_2, CO and CH_4).

This low loss balance enabled to consider the carbon equivalent of quantified compounds by HPLC-RI and GC-FID in the liquid phases (Table 4). In case of the mixture A, only 37.1 wt% of C have been identified by these techniques in the liquid phase compared to the 71.3 wt% of C identified by TOC and CHONS analysis. This balance suggests that remaining carbon may be considered as non-quantified heavy molecular weight products solubilized in the liquid phase and represented by SEC-RI analysis (Figure 1).

Thus, considering carbon balance obtained from Glu/Gua/Fur conversion, it has been observed that guaiacol clearly limited the solid formation while the GC/HPLC non-quantified carbon increased to 60.9 wt% (Table 4). This is consistent with the high rate of soluble macromolecules detected by SEC-RI (Figure 1). On the contrary, the solid residues (coke onto the catalyst or recovered in the reactor) obtained from Glu/Fur/AA mixture contained more than 75 wt% of the initial introduced carbon.

As shown in Table 4, equivalent carbon in the gaseous phase was quantitatively negligible in comparison with the liquid phase. Major released gaseous species (CO_2 and CO) were mainly produced by D-glucose while furfural and guaiacol produced a few CH_4 (see Supplementary Fig. S1).

Considering previous D-glucose, furfural and guaiacol conversion schemes, distribution of GC quantified products according to reaction pathways and chemical functions in the liquid effluents are reported in Supplementary data (Supplementary Fig. S3)

This original approach provided by a multi-scale analytical strategy demonstrated the cross reaction between D-glucose and furfural leading to the production of heavy molecular weight compounds. Without guaiacol in the feed those compounds are precursors of solid residues [23]. To improve the system description, this study needs to be completed by varying the operating conditions such as reaction time and temperature (Supplementary Fig. S15 presents a summary scheme of parts 3.2 and 3.3).

3.2. Effect of the reaction time on the mixture A catalytic hydroconversion

In this part, the effect of the reaction time on the catalytic hydroconversion of *Mixture A* is investigated at 250°C from t_0 (heating period of the reactor) to 180 min. Figure 2 [A] reports the recovered amount of liquid, gas and solid effluents of each experimental test.

Before 45 min of reaction, the solid production represented less than 3 wt% of recovered phases whereas the sum of the liquid phases remained stable. After 45 min, solid

deposition onto the reactor and the catalyst increased to reach 15.1 g at 3 h. This trend was heightened at 180 min while no liquid organic phase has been recovered (orange square dots on Figure 2 [A]). Experimental losses were systematically inferior to 10 wt%. Complete experimental balances as well as hydrogen consumptions are available in Supplementary data (Supplementary Table S2 and Fig. S7).

The carbon balance illustrated in Figure 2 [B] was obtained considering the HPLC-RI and GC-FID quantified carbon in the liquid phases (sum quantification from the three liquid phases). It indicates that the worst quantification in the liquid phases was reached at 45 min. Above 60 min of reaction, the solid production increased as well as the quantification in the liquid phases. In addition, the gas production (mainly composed by CO, CO_2 and CH_4) represented only from 0.4 to 2.3 wt% of C.

The evolution of the main chemical functions and reactions observed for the products of catalytic hydroconversion of mixture A, according to the residence time, are reported in Supplementary data (Supplementary Fig. S8). It can be noted that at the early stages of the reaction, dehydration is the predominant reaction. Those reactions were likely arising from D-glucose conversion [23] even during the heating time (t0). During this period, carbonyls (including furanic species) and carboxylic acids (such as levulinic acid or lactic acid) were widely produced. Thus, GC analyzed compounds in the liquid phases were mainly composed by carbonyls and acids progressively converted into alcohols and hydrocarbons. This evolution is consistent with the H_2 consumption and appeared to arise between 45 and 60 min of reaction (Supplementary Table S2).

Nevertheless, considering the carbon balances (Figure 2 [B]), the GC and HPLC quantification represents only a fraction of the organic compounds produced. An additional representation of the evolution of the liquid phases is given by normalized SEC-RI (see Figure 3) and SEC-UV 254 nm (Supplementary Fig. S9) elugrams.

Heavy compounds reached their maximum intensity within 15 min concomitantly with D-glucose and furfural conversion. As previously observed [23], D-glucose was totally converted after the heating period (t0) contributing to the production of heavy molecular weight compounds. Furfural, totally converted within 45 min, is also responsible for this production. As reported in Figure 3 [B], products were likely soluble in the organic phases until 45 min of reaction since a few solid residues were observed. With the increase of the reaction time, the recovered organic phases decreased (See Figure 2 [A]) and completely disappeared at 180 min of reaction time. In the aqueous phase (Figure 3 [A]), two intense peaks were detected: a 248 $g.mol^{-1}$ PS eq. peak was ascribed to an unidentified D-glucose conversion product and a 160 $g.mol^{-1}$ PS eq. peak belonging to 1,2-benzenediol. The evolution of the latter peak is linked to the recovered guaiacol mass (quantified by GC-FID) as illustrated by Figure 4. In the feed, 45 g of guaiacol was introduced.

Figure 4 also reports the ratio between GC-quantified guaiacol products carbon equivalent and carbon equivalent released from guaiacol conversion. GC-quantifiable guaiacol products were 1,2-benzenediol and phenol. At the very beginning of the reaction, less than 1 % of introduced guaiacol was converted. Nevertheless, only 11.7 wt% of the released carbon was actually quantified by GC-FID. Further, more than 45 % of guaiacol was converted but less than 1 wt% of the released carbon was actually ascribed to it GC-quantifiable products. Finally, from 45 min, guaiacol conversion significantly decreased (as shown by a higher GC-FID quantification of this compound in Figure 4) and a growth of it products was observed.

Three chemical pathways might describe guaiacol behavior during the catalytic hydroconversion:

- Firstly, guaiacol can be converted into GC-quantifiable hydroconversion products (such as phenol or 1,2-benzenediol). If so, the sum of carbon equivalent of those products would be necessarily equal to the sum of carbon equivalent from the guaiacol conversion.
- Guaiacol or its products can react with heavy molecular weight compounds product precursors issued from D-glucose and furfural (for example in Figure 4 through the formation of a hemi-acetal by nucleophilic addition followed by dehydration). For a high guaiacol conversion rate, only few products will be quantified by GC. In this case, the sum of carbon equivalent of GC-quantifiable products is away from the sum of carbon equivalent from the guaiacol conversion.
- At last, guaiacol could be not affected by the hydroconversion conditions and remains in the organic phase. In this last case, a low guaiacol conversion rate as well as low by-products detection would be observed.

Referring to Figure 4, until 45 min of reaction, guaiacol quantification reached 19.4 g (i.e. 56 % of conversion) while less than 0.3 wt% of C of its products were quantified by GC-FID. This yield suggests that guaiacol or its conversion products readily reacted with D-glucose and furfural macromolecule precursors [23] to produce heavier structures still soluble in the organic phase. Regarding the experimental balances (Figure 2 [A]), this pathway seems to prevent the solid residues production observed when increasing the amount of soluble macromolecule in the organic phase (Figure 3 [B]). Indeed, between 45 min and 60 min, recovered guaiacol mass increased while the yields of GC-quantifiable products slightly increased. This trend suggests that soluble heavy molecular weight compounds initially formed with guaiacol were further converted by hydrogenolysis. Then, beyond 45 min of reaction, residual macromolecules were no longer soluble in the organic phase and precipitated resulting in the decrease of intensities of SEC-RI signal (Figure 3 [B]).

In order to confirm the guaiacol role, a *Mixture B* (see feed compositions in Table 1) has been converted under similar operating conditions. This mixture, in which 15 % of

guaiacol were replaced by n-hexadecane, produced 50 wt% solid more than Mixture A. As previously studied [23], those structures were observed from D-glucose hydroconversion suggesting chemical pathway involving furanic species (i.e. 5-HMF, furfural, etc.) production subsequently converted into macromolecules precursors. From Mixture B hydroconversion, liquid phase analysis revealed that a higher amount of dehydration reactions occurred. Those reactions were identified to promote the production of macromolecules.

Solid residues were highly made of carbon (up to 70 wt% of C). Reported ^{13}C NMR in Supplementary data (Supplementary Fig. S10), confirms that Mixture B solids residues were containing less aromatics and alkyl compounds and more carbonyl functions. Considering the high content of oxygen in the solid residues (25 wt% on average) and their ^{13}C NMR analysis, the precipitation suggests a change of the organic phase, like for instance a decrease of the polarity during the hydroconversion for long reaction time. Atomic carbon ratios did not change significantly with reaction time.

As an intermediate conclusion, these results highlight the fast conversion of D-glucose and furfural leading to macromolecules precursors. It has been observed that guaiacol and its products led to the formation of larger soluble macromolecules until 45 min of reaction. Afterwards, the GC analysis revealed the recovery of guaiacol and it product (1,2-benzenediol) simultaneously with the precipitation of macromolecules.

3.3. Effect of temperature on the mixture A catalytic hydroconversion

To improve the understanding of *Mixture A* catalytic hydroconversion, the effect of temperature was investigated. Thus, studied temperature were 200, 250 and 300°C. Complete experimental balances as well as hydrogen consumptions are reported in Supplementary data (Supplementary Table S3 and Fig. S11). Figure 5 [A] and [B] displays respectively the experimental and carbon balances of those three experiments.

At the lowest temperature, the liquid phases were mainly obtained (about 85 wt%), containing most of the initially introduced carbon (i.e. 58.9 g verified by CHONS elementary analysis). Nevertheless, as indicated in Figure 5 [B], carbon content quantified by GC in the liquid phases was low. Temperature appears to strongly affect the effluent distribution by producing a larger amount of solid residues and gas from 250°C (Figure 5 [A]). From the GC-FID analysis, reported in Supplementary data (Supplementary Fig. S12), we can observe that higher temperature led to an increase of the alcohols function production mostly from hydrogenolysis reaction. This will be further discussed considering the guaiacol conversion.

From a global point of view, SEC-RI analysis (Figure 6) and carbon balances (Figure 5 [B]) revealed that soluble macromolecules formed the main part of the products.

Those SEC-RI analyses (SEC-UV 254 nm reported in supplementary Fig. S13) also indicated the chemical pathways modifications between 250 and 300°C involving the disappearance of a 248 $g.mol^{-1}$ PS eq. peak (supposed from D-glucose products) subsequently replaced by a 160 $g.mol^{-1}$ PS eq. peak (ascribed to 1,2-benzenediol). Those two peaks were already observed during the previous reaction time. This behavior modification is confirmed regarding the recovered guaiacol mass and guaiacol products quantified by GC reported in Table 5.

As previously discussed, while the same quantity of guaiacol was recovered, its role was completely dependent on the temperature. At 200°C, only 0.4 wt% of the carbon equivalent from guaiacol conversion was quantified. This suggests that it reacted with D-glucose and furfural macromolecules precursors. This result may explain the absence of solid residues in the resulting effluent. Further, 250°C seems to be the breaking point favoring the production of solid residues but still for a low amount of guaiacol hydroconversion products. Finally, at 300°C, guaiacol was converted up to 17 wt% of C of the carbon equivalent into aromatic products (as 1,2-benzenediol). Then, the guaiacol conversion limited the macromolecules solubilization and promoted the solid formation. Furthermore, decarbonylation and decarboxylation reactions increased between 250 and 300°C (Supplementary Fig. S12). This may lead to the production of less polar high molecular weight compounds in the liquid phase which were less prone to react with guaiacol (and it product) and precipitated.

To get an insight of produced solids at 250 and 300°C, ^{13}C NMR analysis were performed (Supplementary Fig. S14). The ^{13}C NMR spectra obtained for the two residues confirm the previous observations. Indeed, although solid residues contain mostly aromatic and aliphatic functional groups, temperature clearly affects the structures. Then, aromatic groups dropped from 65 % carbon atoms at 250°C to 57 % carbon atoms at 300°C suggesting that guaiacol (or it products as 1,2-benzenediol) was slightly less involved in the soluble macromolecules formation at higher temperatures. The decrease of the polarity of the solid precursors is in agreement with the elementary analysis of solids containing 40.5 and 33.5 wt% of oxygen respectively at 250 and 300°C as previously suggested in the case of coal derived liquids [39].

Following the previous studies, the temperature is also a key parameter for this process. In every case, D-glucose and furfural were proven to be very reactive compounds mainly leading to macromolecules precursors. In order to limit the solid production, the mixture should be processed at low temperature to initially promote the reaction of guaiacol with macromolecules precursors. In this way, those structures are stabilized in the organic phase.

4. Conclusions

Furfural and D-glucose catalytic hydroconversion led to a wide range of soluble macromolecules or precursors that were prone to precipitate in a water medium. Guaiacol addition limits the solid formation and lead to larger macromolecules (up to 5,000 g.mol^{-1}) soluble in the organic phase. This phenomenon was mainly observed at low temperature and short reaction time suggesting that guaiacol was not converted into its light usual hydroconversion products. At high temperature or long reaction time guaiacol was mainly converted into light aromatic compounds and contributed in a lesser extent to the macromolecule solubilization. This was observed simultaneously with the production of solid residues.

The control of the macromolecules and subsequent solid production remains the main drawback of the industrial bio-oil hydroconversion process. Moreover, in order to go further and to better control the contact time and the temperature before reaction, a similar study could be done in continuous reactor including an on-line sampling system. In the same operating conditions and thanks to the developed analytical strategy (i.e. SEC, ^{13}C NMR, GC, HPLC), the effect of the presence of guaiacol during the bio-oil hydroconversion was studied and will be the topic of a following paper.

5. Appendix

Supplementary data associated with this article can be found, in the online version.

6. Acknowledgments

Authors thanks for fruitful discussions and reviews of this paper: F. Albrieux, N. Charon, A. Le Masle and V. Souchon from IFPEN. In addition, M. Ozagac is grateful to F. Neyret-Martinez, R. Comte and S. Sivault.

7. References

[1] A. V. Bridgwater, Review of fast pyrolysis of biomass and product upgrading, Biomass Bioener. 38 (2012) 68-94

[2] E. Furimsky, Catalytic hydrodeoxygenation, Appl. Catal., A. 199 (2000) 147-190

[3] A. Oasmaa and P. Peacocke, A guide to physical property characterisation of biomass-derived fast pyrolysis liquids, VTT Publications 731 (2010) Espoo

[4] D. C. Elliott, Historical developments in hydroprocessing bio-oils, Energ. Fuel. 21 (2007) 1792-1815

[5] R. H. Venderbosch, H. J. Heeres, Pyrolysis oil stabilisation by catalytic hydrotreatment, in: Biofuel's engineering process technology, Dr. Marco Aurelio Dos Santos Bernardes (Ed.), (2011) 385-410, Rijeka

[6] R. H. Venderbosch, A. R., Ardiyanti, J. Wildschut, A. Oasmaa, H. J. Heeres, Stabilization of biomass-derived pyrolysis oils, J. Chem. Tech. Biotechnol. 85 (2010) 674-686

[7] D. C. Elliott, S. J. Lee, T. R. Hart, Stabilization of Fast Pyrolysis Oil: Post Processing, PNNL report – 21549 (2012) Washington

[8] E. Hoekstra, S. R. A. Kersten, A. Tudos, D. Meier, K. J. A. Hogendoorn, Possibilities and pitfalls in analyzing (upgraded) pyrolysis oil by size exclusion chromatography (SEC), J. Anal. Appl. Pyrol. 91 (2011) 76-88

[9] M. Castellví Barnés, J. P. Lange, G. van Rossum, S. R. A. Kersten, A new approach for bio-oil characterization based on gel permeation chromatography preparative fractionation, J. Anal. Appl. Pyrol. 113 (2015) 444-453

[10] R. Bayerbach, V. D. Nguyen, U. Schurr, D. Meier, Characterization of the water-insoluble fraction from fast pyrolysis liquids (pyrolytic lignin): Part III. Molar mass characteristics by SEC, MALDI-TOF-MS, LDI-TOF-MS, and Py-FIMS, J. Anal. Appl. Pyrol. 77 (2006) 95-101

[11] T. A. Milne, F. Agblevor, M. Davis, S. Deutch, D. Johnson, Development in thermal biomass conversion, Blackie Academic and Professional (1997) London

[12] J. H. Marsman, J. Wildschut, F. Mahfud, H. J. Heeres, Identification of components in fast pyrolysis oil and upgraded products by comprehensive two-dimensional gas chromatography and flame ionisation detection, J. Chrom. 1150 (2007) 21-27

[13] H. Yang, R. Yan, H. Chen, D. H. Lee, C. Zheng, Characteristics of hemicellulose, cellulose and lignin pyrolysis, Fuel 86 (2007) 1781–1788

[14] R. Gunawan, X. Li, A. Larcher, X. Hu, D. Mourant, W. Chaiwat, H. Wu, C. Zhu Li, Hydrolysis and glycosidation of sugars during the esterification of fast pyrolysis bio-oil, Fuel 95 (2012) 146-151

[15] A. B. Bindwal, P. D. Vaidya, Kinetics of aqueous-phase hydrogenation of levoglucosan over Ru/C catalyst, Ind. Eng. Chem. Res 52 (2013) 17781-17789

[16] T. P. Vispute, G. W. Huber, Production of hydrogen, alkanes and polyols by aqueous phase processing of wood-derived pyrolysis oils, Green Chem. 11 (2009) 1433-1445

[17] S. Helle, N. M. Bennett, K. Lau, J. H. Matsuib, S. J. B. Duffb, A kinetic model for production of glucose by hydrolysis of levoglucosan and cellobiosan from pyrolysis oil, Carbohydr. Res. 342 (2007) 2365–2370

[18] R. Mariscal, P. Maireles-Torres, M. Ojeda, I. Sádaba, M. López Granados, Furfural: a renewable and versatile platform molecule for the synthesis of chemicals and fuels, Energ. Environ. Sci. 9 (2016) 1144-1189

[19] F.-X. Collard and J. Blin A review on pyrolysis of biomass constituents: Mechanisms and composition of the products obtained from the conversion of cellulose, hemicelluloses and lignin, Renew. Sustain. Energ. Rev. 38 (2014) 594-608

[20] R. Bayerbach, D. Meier, Characterization of the water-insoluble fraction from fast pyrolysis liquids (pyrolytic lignin). Part IV: Structure elucidation of oligomeric molecules, J. Anal. Appl. Pyrolysis 85 (2009) 98–107

[21] D. C. Elliott, T. R. Hart, Catalytic hydroprocessing of chemical models for bio-oil, Energ. Fuel 23 (2009) 631-637

[22] R. C. Runnebaum, T. Nimmanwudipong, D. E. Block, B. C. Gates, Catalytic conversion of compounds representative of lignin-derived bio-oils: a reaction network for Guaiacol, anisole, 4-methylanisole, and cyclohexanone conversion catalysed by Pt/[gamma]-Al_2O_3, Catal. Sci. Technol. 2 (2012) 113-118

[23] M. Ozagac, C. Bertino-Ghera, D. Uzio, M. Rivallan, D. Laurenti, C. Geantet, Biomass Bioener. (2016) (Submitted)

[24] C. Boscagli, K. Raffelt, T. A. Zevaco, W. Olbrich, T. N. Otto, J. Sauer, J.-D. Grunwaldt, Mild hydrotreatment of the light fraction of fast-pyrolysis oil produced from straw over nickel-based catalysts, Biomass Bioener. 83 (2015) 525–538

[25] A. R. Ardiyanti, S. A. Khromova, R. H. Venderbosch, V. A. Yakovlev, I. V. Meliín-Cabrera, H. J. Heeres, Catalytic hydrotreatment of fast pyrolysis oil using bimetallic Ni–Cu catalysts on various supports, Appl. Catal., A. 449 (2012) 121-130

[26] A. R. Ardiyanti, M. V. Bykova, S. A. Khromova, W. Yin, R. H. Venderbosch, V. A. Yakovlev, H. J. Heeres, Ni-Based Catalysts for the Hydrotreatment of Fast Pyrolysis Oil, Energ. Fuel 30 (2016) 1544-1554

[27] J. T. Scanlon and D. E. Willis, Calculation of flame ionization detector relative response factors using the effective carbon number concept, J. Chromatogr. Sci. 23 (1985) 333-340

[28] J. Wildschut, J. Arentz, C. B. Rasrendra, R. H. Venderbosch, H. J. Heeres, Catalytic hydrotreatment of fast pyrolysis oil: Model studies on reaction pathways for the carbohydrate fraction, Environ. Progr. Sustain. Energ. 28 (2009) 450-460

[29] L. Vilcocq, A. Cabiac, C. Especel, E. Guillon, D. Duprez, Transformation of sorbitol to biofuels by heterogeneous catalysis: chemical and industrial considerations, Oil Gas Sci. Tech. 68 (2013) 841-860

[30] S. Sitthisa, T. Pham, T. Prasomsri, T, Sooknoi, R. G. Mallinson, D. E. Resasco, Conversion of furfural and 2-methylpentanal on Pd/SiO_2 and $Pd-Cu/SiO_2$ catalysts, J. Catal. 280 (2011), 17-27

[31] S. Sitthisa, D. E. Resasco, Hydrodeoxygenation of furfural over supported metal catalysts: a comparative study of Cu, Pd and Ni, Catal. Lett. 141 (2011), 784-791

[32] S. Sitthisa, T. Sooknoi, Y. Ma, P. B. Balbuena, D. E. Resasco, Kinetics and mechanism of hydrogenation of furfural on Cu/SiO_2 catalysts, J. Catal. 277 (2011) 1-13

[33] E. Laurent, B. Delmon, Study of the hydrodeoxygenation of carbonyl, catalytic and guaiacyl groups over sulfided $CoMo/Al_2O_3$ and $NiMo/Al_2O_3$ catalysts: I. Catalytic reaction schemes, Appl. Catal., A. 109 (1994) 77-96

[34] E. Laurent, B. Delmon, Study of the hydrodeoxygenation of carbonyl, carboxylic and guaiacyl groups over sulfided $CoMo/Al_2O_3$ and $NiMo/Al_2O_3$ catalyst: II. Influence of water, ammonia and hydrogen sulfide, Appl. Catal., A. 109 (1994) 97-115

[35] V. N. Bui, D. Laurenti, P. Afanasiev, C. Geantet, Hydrodeoxygenation of guaiacol with CoMo catalysts. Part I: Promoting effect of cobalt on HDO selectivity and activity, Appl. Catal. B Environ. 101 (2011) 239-245

[36] V. N. Bui, D. Laurenti, P. Delichère, C. Geantet, Hydrodeoxygenation of guaiacol: Part II: support effect for CoMoS catalysts on HDO activity and selectivity, Appl. Catal. B Environ. 101 (2011) 246-255

[37] S. Li, S. Zhang, F. Feng, Y. Yan, Coke formation in the catalytic cracking of bio-oil model compounds, Environ. Progr. Sustain. Energ. 34 (2015) 240–247

[38] M. V. Bykova, O. A. Bulavchenko, D. Yu Ermakov, M. Yu Lebedev, V. A. Yakovlev, V. N. Parmon, Guaiacol hydrodeoxygenation in the presence of Ni-containing catalysts, Catal. Ind. 3 (2011) 15-22

[39] J. Stihle, D. Uzio, C. Lorentz, N. Charon, J. Ponthus, C. Geantet, Detailed characterization of coal-derived liquids from direct coal liquefaction on supported catalysts, Fuel 95 (2012) 79-87

Table

	Single reactants			Ternary mixtures				Four-compound mixtures	
	Gua	**Fur**	**Glu**	**Glu/Fur/ AA**	**Glu/Gua/ AA**	**Gua/Fur/ AA**	**Glu/Gua/Fur**	**Mixture A**	**Mixture B**
Water	30	30	30	30	30	30	30	30	30
D-Glucose	0	0	20	20	20	0	20	20	20
Furfural	0	13	0	13	0	13	13	13	13
Acetic acid	0	0	0	7	7	7	0	7	7
Guaiacol	30	0	0	0	30	30	30	30	15
n-C16	40	57	50	30	13	20	7	0	15

Table 1 : Composition in wt% of the single, three and four-compound (ternary) mixtures

		Single reactants			Ternary mixtures				
		Gua	Fur	Glu	Glu/Fur /AA	Glu/Gua /AA	Gua/Fur /AA	Glu/Gua/ Fur	Mixture A
Inlet	Liquid phase (g)	150	150	150	150	150	150	150	150
	Reduced catalyst (g)	14.1	14.3	14.5	14.2	14.1	14.2	14.1	14.3
	Introduced H_2 (g)	2.3	3.6	2.5	2.7	2.1	3.2	2.9	2.2
Outlet	Liquid phase (g)	151.9	142.9	105.7	85.9	140.4	149.4	139.3	108.8
	Gaseous phase without H_2 (g)	0	0.8	2.7	3.1	2.9	0.2	3.1	4.1
	Solid residues (g)	0	0	11.9	22.1	1.8	1.3	0.7	11.2
	Catalyst (g)	14.9	15.7	18.5	22.3	15.3	15	15.9	21
	Experimental loss (wt%)	-1.4	3.9	15.7	18.7	2.5	-0.2	3.7	11.7
	H_2 consumption /introduced	0.2	0.5	0.2	0.1	0.1	0.4	0.4	0.1
	H_2 consumption /introduced reactant (mol/mol)	0.5	4.1	1.3	0.4	0.2	0.8	0.7	0.1

Table 2 : Mass balances of single reactants, ternary mixtures and Mixture A (Gua/Fur/AA/Glu) hydroconversion at 250°C during 1 h

	Feed	Recovered fractions						Carbon Balance Loss
	Mixture A	Liquid organic phase	Liquid aqueous phase	Washed liquid phase	Gas phase	Catalyst	Solid residues	
Weight of equivalent carbon (g)	**58.9**	2.2	4.9	34.9	1.2	7.0	7.8	**- 0.9**
Percentage of recovered equivalent carbon (wt %)	-	3.7	8.3	59.3	2.0	12.0	13.3	**- 1.5**

Table 3 : Global carbon balance of Mixture A (Gua/Fur/AA/Glu) catalytic hydroconversion at 250°C during 1 h

	Single reactants			Ternary mixtures				Mixture A
	Gua	Fur	Glu	Glu/Fur/AA	Glu/Gua/AA	Gua/Fur/AA	Glu/Gua/F	
Inlet (gC)	30.5	12.5	12.0	28.4	46.7	46.9	54.7	58.9
Liquid phases (wt%)	83.1	38.2	5.9	13,7	70.0	64.3	35.5	37.1
Gaseous phase (wt%)	0.0	1.8	6.5	3,9	1.9	0.3	1.8	2.0
Catalyst (wt%)	0.0	5.8	15.5	11,7	1.5	0.6	1.8	12.0
Solid residues (wt%)	0.0	0.0	44.6	65,1	0.0	0.0	0.0	13.3
Not quantified (wt%)	16.9	54.2	27.5	5,5	26.6	34.7	60.9	**35.8**

Table 4 : Carbon balances of single reactants, ternary mixtures and Mixture A (Gua/Fur/AA/Glu) catalytic hydroconversion at 250°C during 1 h

	200°C	250°C	300°C
Quantified guaiacol (g)	27.2	27.3	29.0
GC quantified guaiacol products carbon / converted (wt%)	0.4	1.1	16.7

Table 5 : Guaiacol recovered mass and GC-quantified products yields as function of temperature (1 h)

Figure

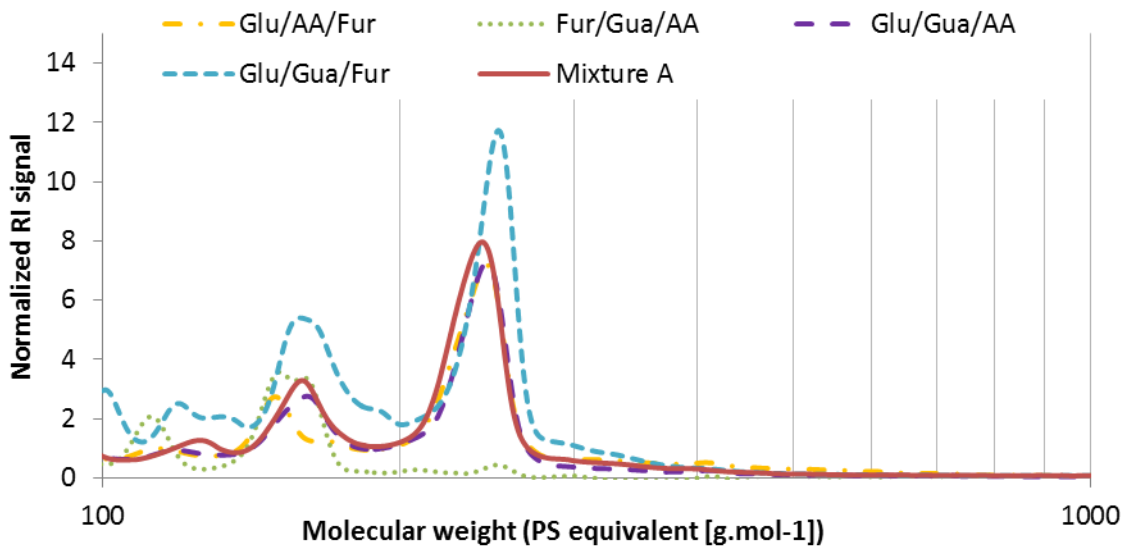

[A]

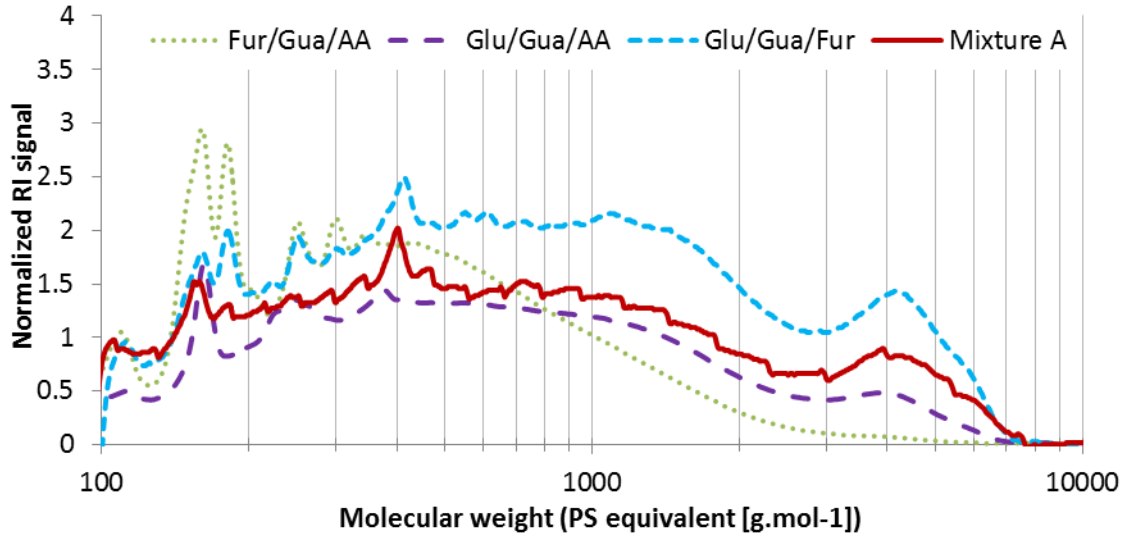

[B]

Figure 1 : Normalized SEC-RI analysis of ternary mixtures and mixture A (Gua/Fur/AA/Glu) catalytic hydroconversion: [A] Aqueous phases, [B] Organic phases

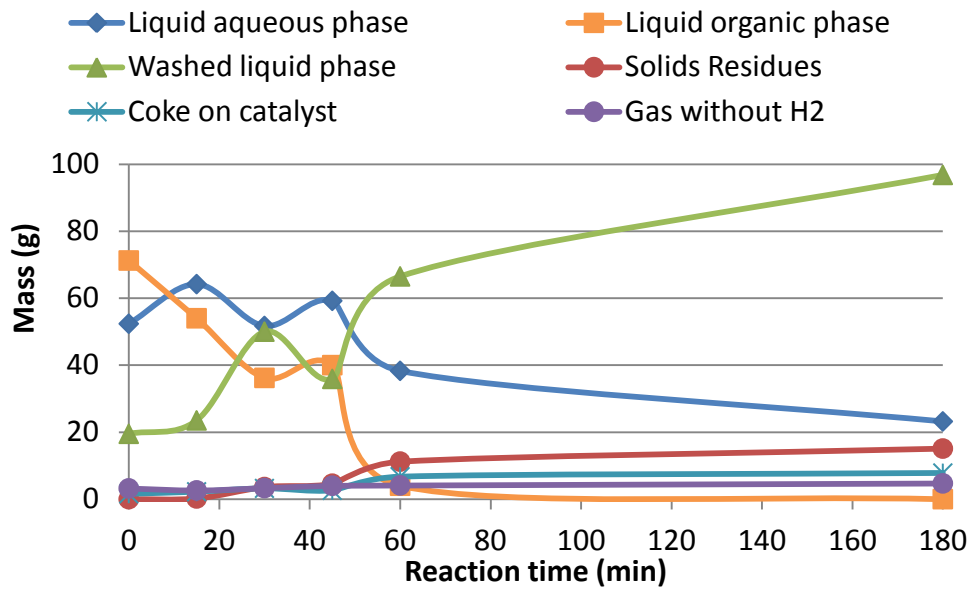

[A]

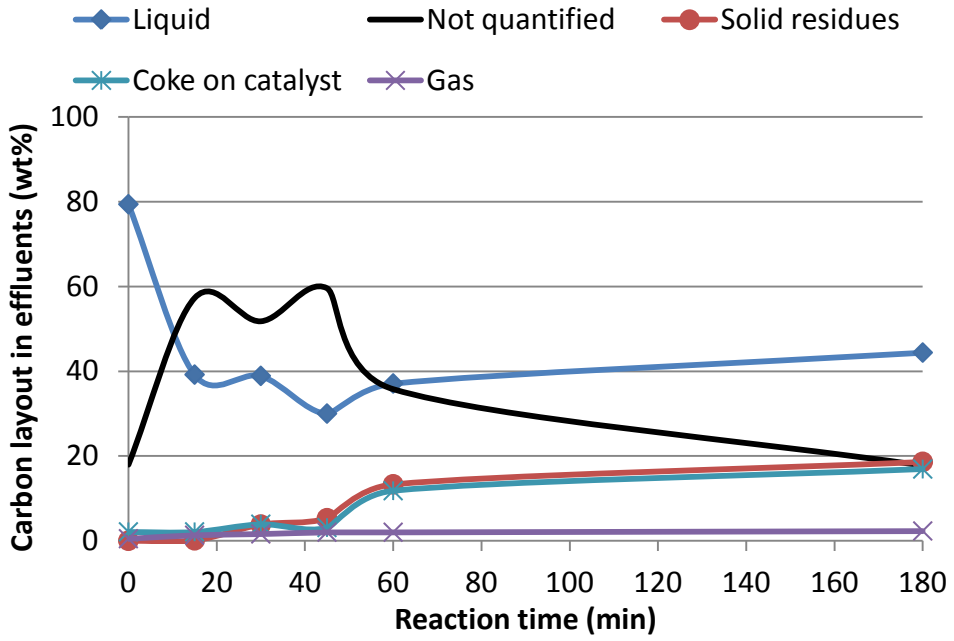

[B]

Figure 2 : [A] Experimental mass and [B] carbon balances of Mixture A (Gua/Fur/AA/Glu) hydroconversion as function of time (250 °C)

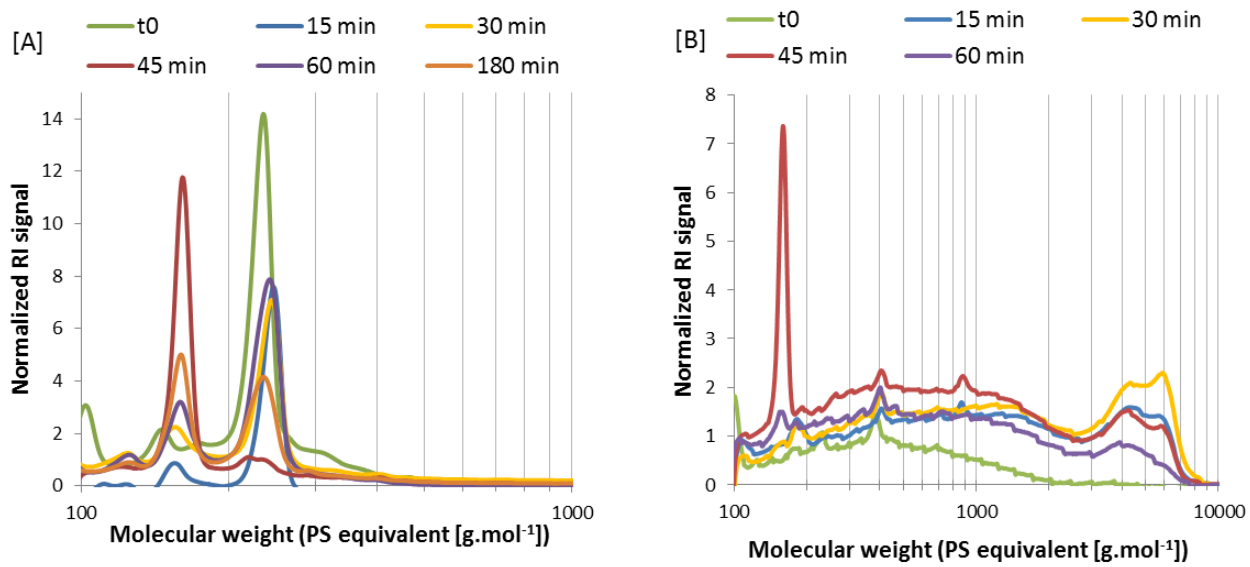

Figure 3 : Normalized SEC-RI analyses of Mixture A (Gua/Fur/AA/Glu) hydroconversion as a function of time (250 °C): [A] Aqueous phases, [B] Organic phases

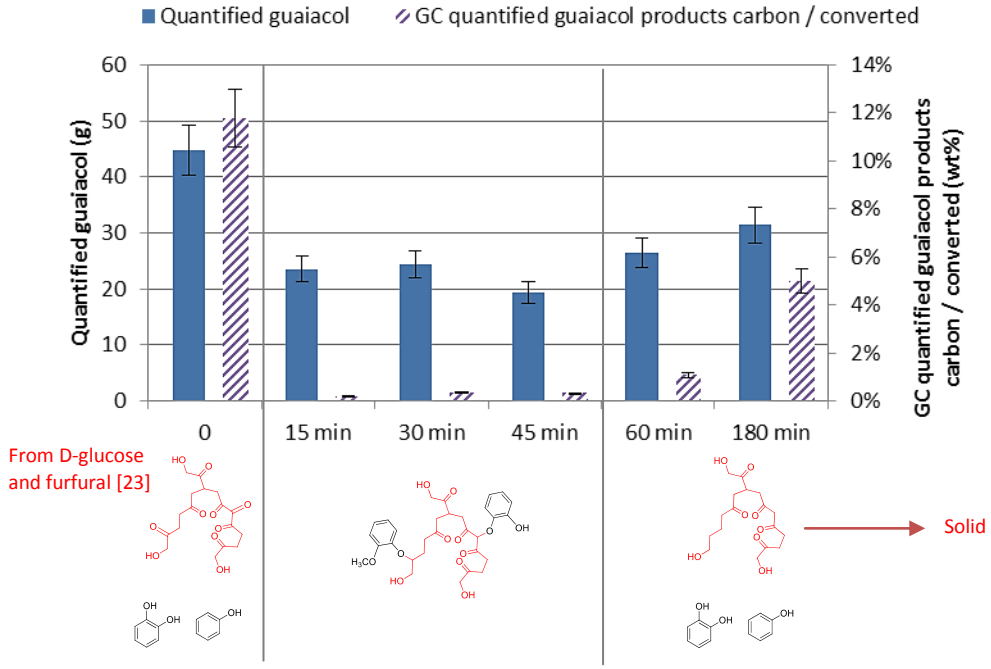

Figure 4 : Recovered guaiacol weight (left axis) and GC-quantified products carbon equivalent (right axis) as a function of time (250 °C)

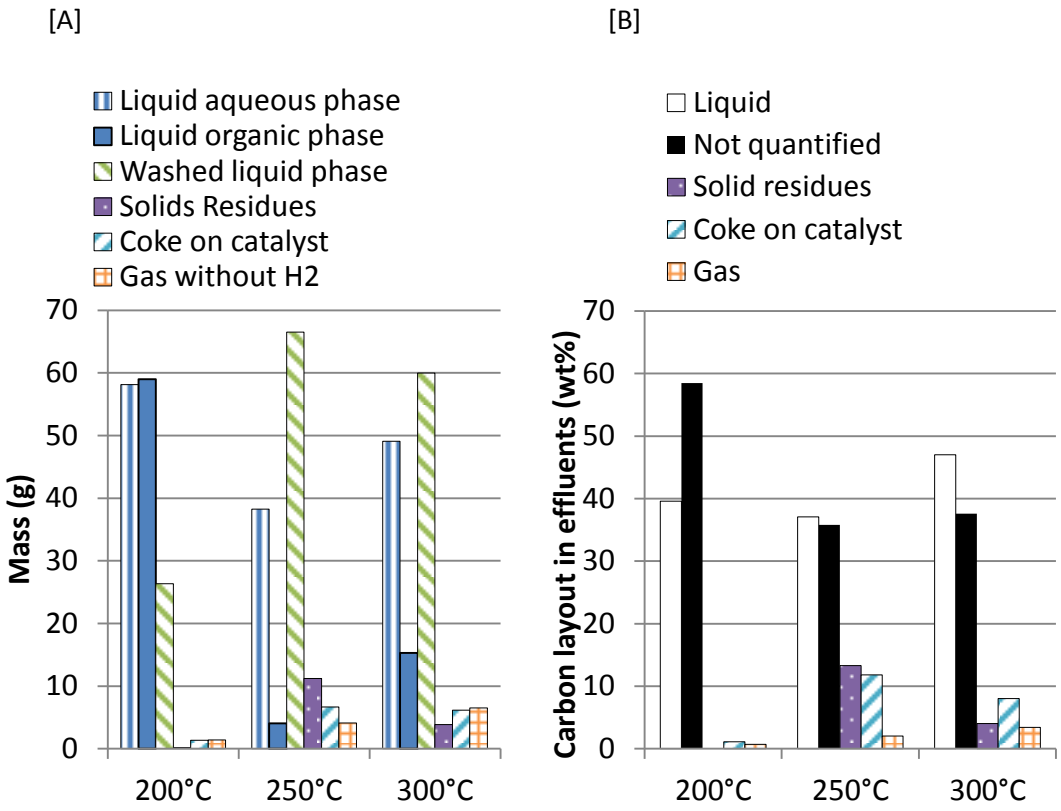

Figure 5 : [A] Experimental mass and [B] carbon balances of Mixture A (Gua/Fur/AA/Glu) hydroconversion as function of temperature (1 h)

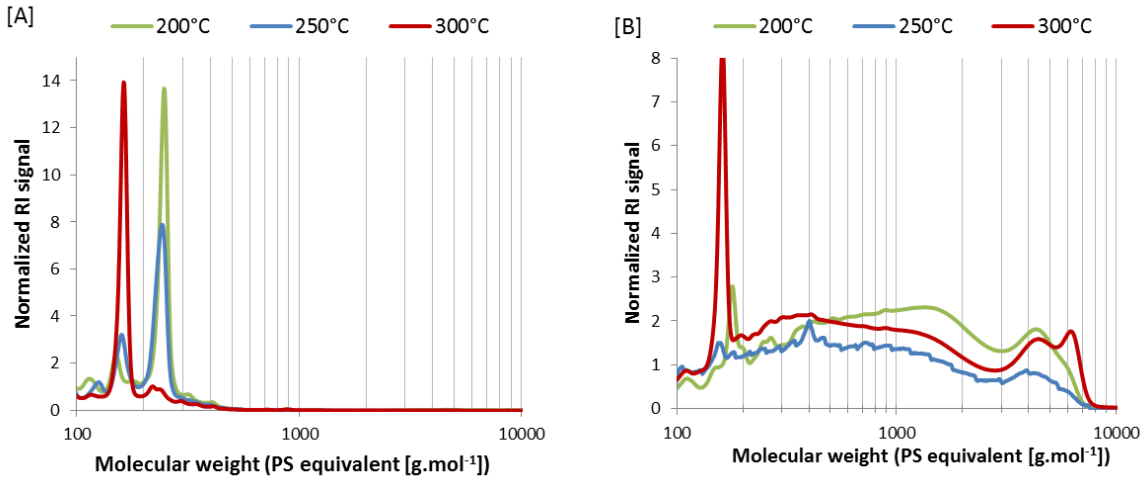

Figure 6 : Normalized SEC-RI analysis of mixture A (Gua/Fur/AA/Glu) catalytic hydroconversion as function of temperature (1 h): [A] Aqueous phases, [B] Organic phases

Impact of guaiacol on the formation of undesired macromolecules during catalytic hydroconversion of bio-oil: a model compounds study

M. Ozagac[a], C. Bertino-Ghera[a,*], D.Uzio[a], M. Rivallan[a], D. Laurenti[b], C. Geantet[b]

[a]*IFP Energies Nouvelles, Rond-point de l'échangeur de Solaize, BP3, 69360 Solaize, France*

[b]*IRCELYON, UMR5256 CNRS-UCBL, 2 avenue A. Einstein, 69626 Villeurbanne cedex, France*

**Corresponding author: celine.bertino-ghera@ifpen.fr*

Supplementary

2. Materials and Methods

2.2. Experimental procedures

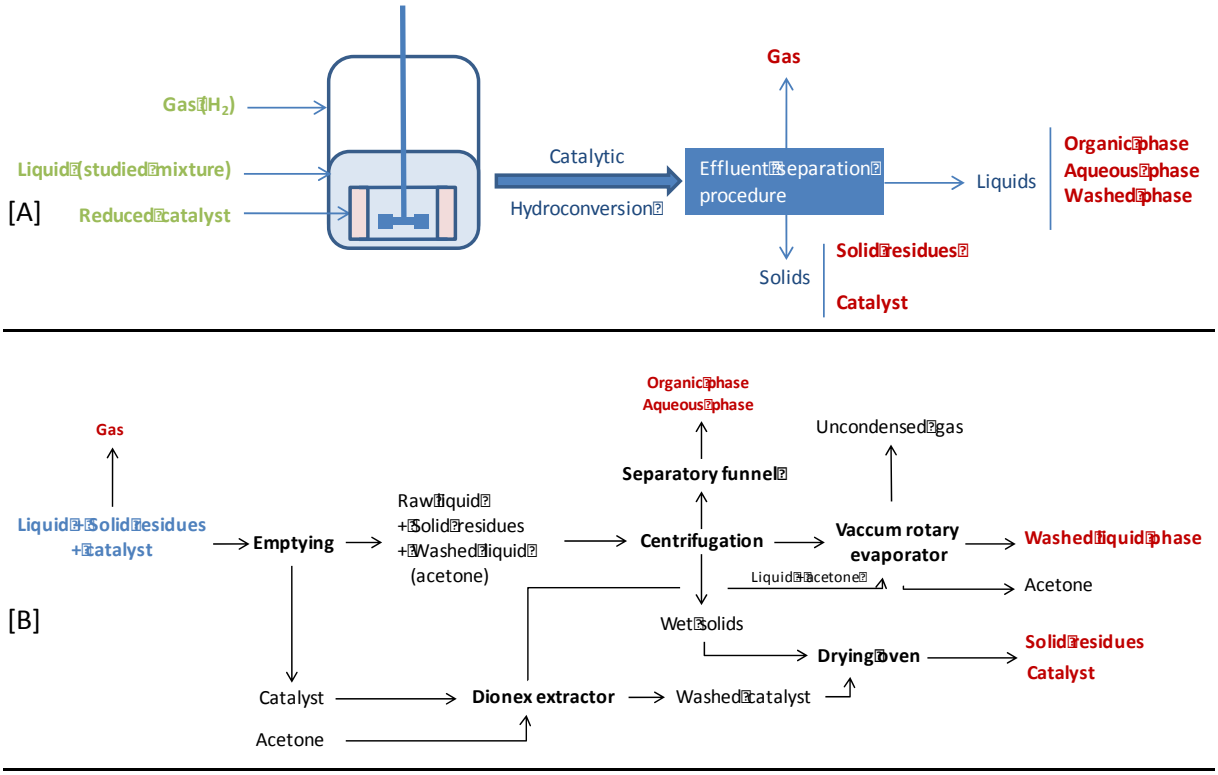

Figure S1 : Schematized experimental procedure [A] global [B] detailed

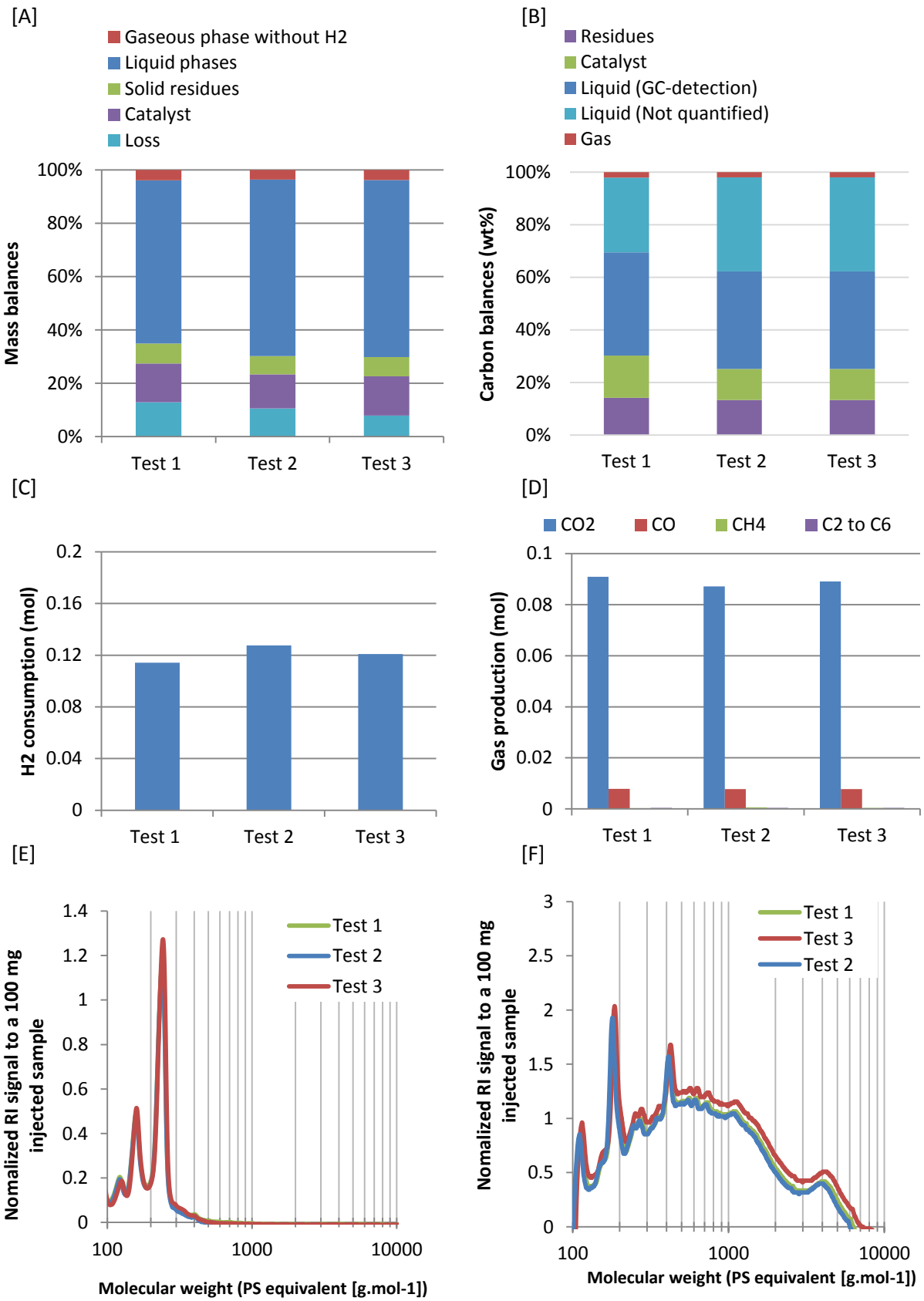

Figure S2 : Repeatability tests of the 5-compound mixture catalytic hydroconversion at 250°C during 1 h. [A] Mass balances, [B] Carbon balances from GC quantification of the liquid phases, [C] Hydrogen consumption, [D] Gas production, [E] SEC-RI analysis of the aqueous phases, [F] SEC-RI analysis of the organic phases

2.3. Analytical procedures

[A]

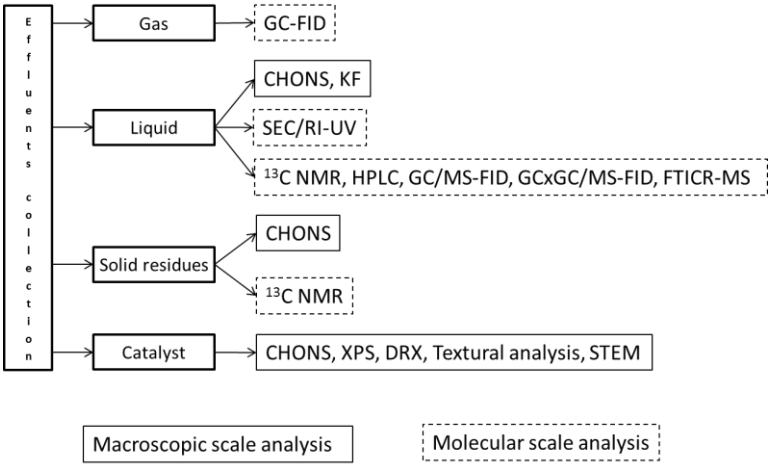

[B]

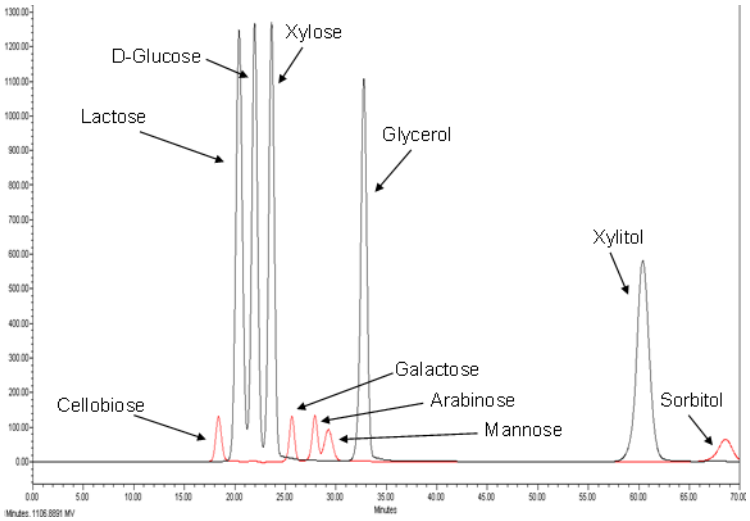

[C]

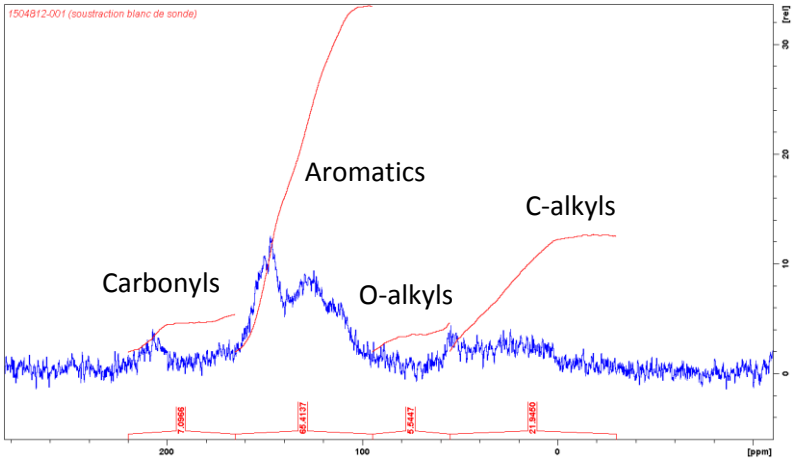

Figure S3 : [A] General analytic procedure, [B] HPLC-RI calibration, [C] Example of a ^{13}C NMR spectra of the solid residue produced from D-glucose at 250°C, 3 h

3. Results and discussion

3.1. Study of the catalytic hydroconversion leading to "Mixture A"

Table S1 reports the mass balances of the two-compound mixtures hydroconversion (250°C – 1 h).

		Binary mixtures				
		G/AA	**G/Gu**	**G/F**	**Gu/F**	**F/AA**
Inlet	Liquid phase (g)	150	150	150	150	150
	Water (wt%)	30	30	30	30	30
	D-Glucose (wt%)	20	20	20	0	0
	Furfural (wt%)	0	0	13	13	13
	Acetic acid (wt%)	7	0	0	0	7
	Guaiacol (wt%)	0	30	0	30	0
	n-C16 (wt%)	43	20	37	27	50
	Reduced catalyst (g)	14.4	14.5	14.2	14.1	14.1
	Introduced H_2 (g)	2.3	2.7	2.5	3.6	3.3
Outlet	Liquid phase (g)	121.6	140.1	80.5	143.7	129.1
	Gaseous phase without H_2 (g)	3.2	2.3	4.4	0.4	0.5
	Solid phase (g)	5.2	0.4	14.3	0.5	1.3
	Catalyst (g)	15.3	15.6	24.9	15.0	15.4
	Experimental loss (wt%)	11.6	4.0	24.3	3.7	11.4
	H_2 consumption/introduced	0.1	0.2	0.2	0.5	0.4
	H_2 consumption / introduced reactant (mol/mol)	0.4	0.6	0.6	1.5	1.8

Index : G (D-glucose), Gu (Guaiacol), F (Furfural), AA (Acetic Acid)

Table S1 : Experimental balances of the two-compounds mixtures hydroconversion (250°C – 1 h)

Gaseous phases analysis from mixtures hydroconversion are reported in Figure S4.

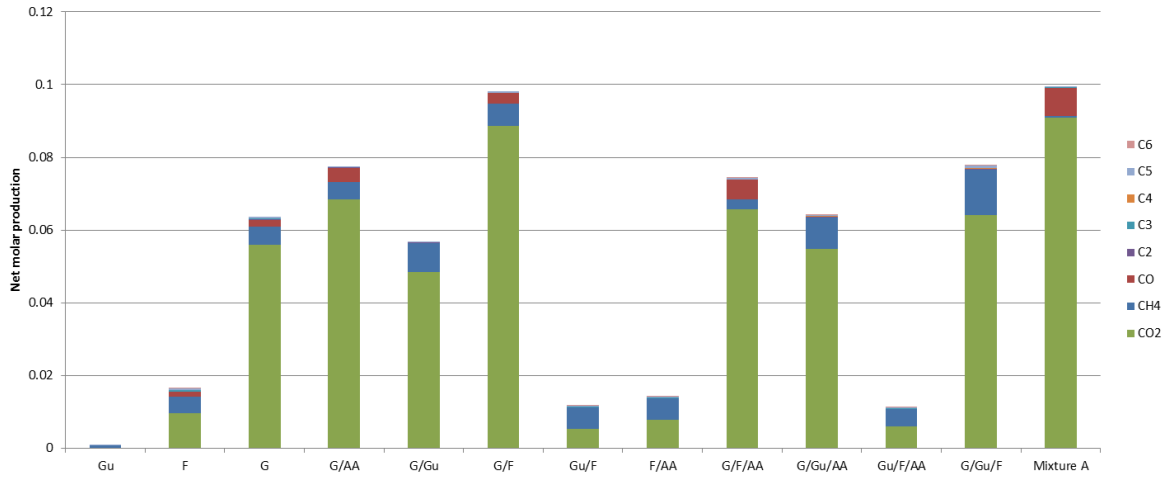

Index : G (D-glucose), Gu (Guaiacol), F (Furfural), AA (Acetic Acid)

Figure S4 : Net molar production in the gas phases from single to mixture A catalytic hydroconversion (250°C – 1 h)

Figure S5 illustrates the reaction scheme for guaiacol catalytic hydroconversion in the operating conditions. 20 compounds were detected by GC-FID analysis of recovered liquid phase.

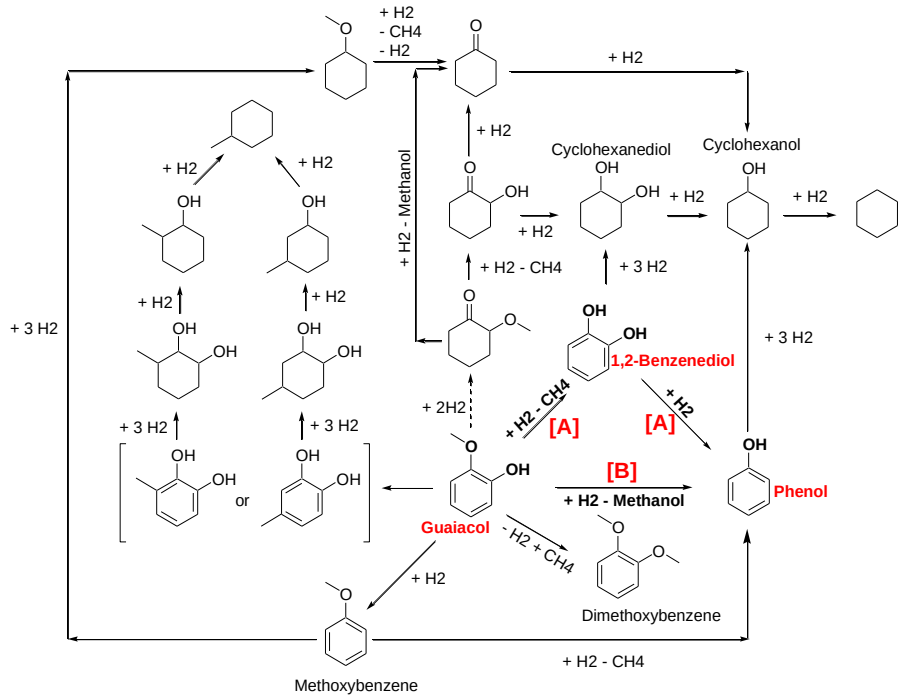

Figure S5: Guaiacol catalytic hydroconversion reaction pathways from GC-FID analysis

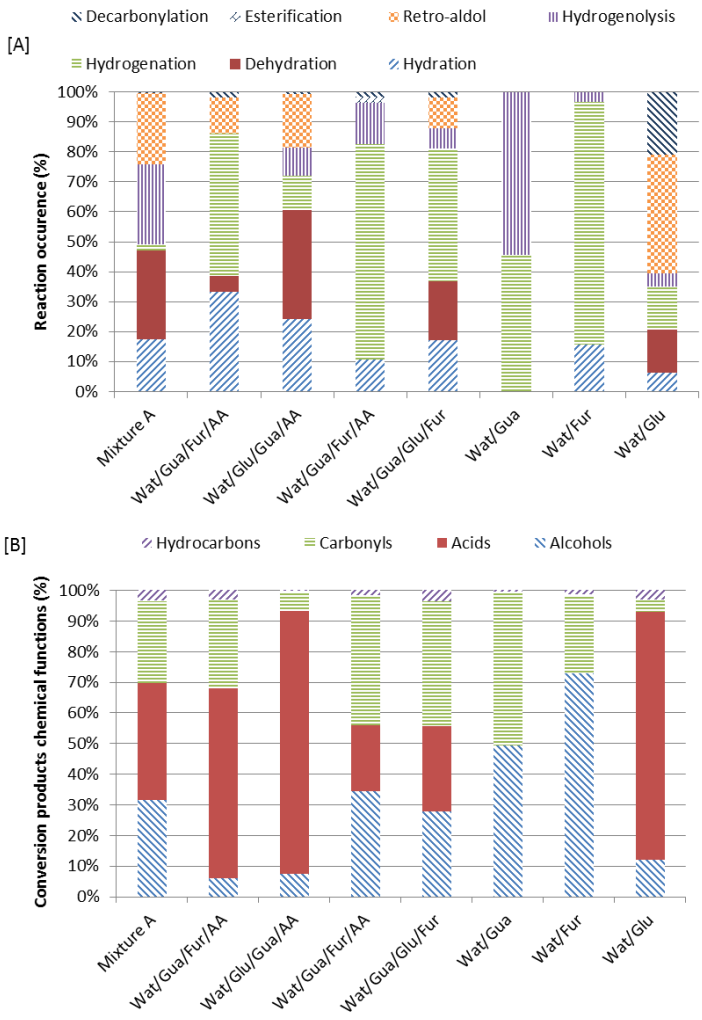

Figure S6 : Mixture A, ternary mixture and single quantified products (250°C – 1 h) [A] Chemical reaction distribution, [B] Chemical functions distribution from Mixture A

Considering previous reaction schemes [23] and Figure S5, distribution of GC detected products according to reaction pathways and chemical functions in the liquid effluents are reported respectively in Figure S6 [A] and [B]. These representations aim at evidencing the main reactions trends observed during the catalytic hydroconversion of *Mixture A*. For Figure S6 [A] simplification, when two pathways were identified to produce the same product, only the main one was considered. For example, 1,2-benzenediol is assumed to be produced only from guaiacol hydrogenolysis and the D-glucose pathway was omitted. For Figure S6 [B], each compound with two oxygenated functions has been accounted twice. The furfural and D-glucose conversion were 100 % for all the experiments. Acetic acid is considered as a reactant but also a D-glucose by-product, therefore no conversion is considered. Those products were quantified by GC and HPLC.

Mixture A conversion products appeared to arise from various chemical pathways producing equally carbonyls, acids and alcohols species. As previously shown, those distributions were

similar to the ternary system Glu/Gua/Fur. Guaiacol involved an increase of hydrogenation reactions (Figure S6 [A]) which is in line with H_2 consumptions reported in Table S1. D-glucose hydroconversion mainly resulted from water-equilibrated reactions (hydration/dehydration/retro-aldol). The presence of acetic acid did not seem to affect much the organic function distributions of GC-FID detected compounds.

3.2. Effect of the reaction time on the mixture A catalytic hydroconversion

Table S2 reports the mass balances.

Reaction time (min)		**0**	**15**	**30**	**45**	**60**	**180**
Inlet	Liquid phase (g)	150	150	150	150	150	150
	Reduced catalyst (g)	14.49	14.1	14	13.9	14.3	14.2
	Introduced H_2 (g)	2.56	1.8	2.2	2.2	2.2	2.5
Outlet	Global liquid phases (g)	143.1	141.7	138	135.1	108.8	120
	• Liquid aqueous phase (g)	52.4	64.2	51.7	59.2	38.3	23.2
	• Liquid organic phase (g)	71.2	54	36.2	40	4	0
	• Washed liquid phase (g)	19.5	23.5	50	35.9	66.5	96.8
	Gaseous phase without H_2 (g)	3.2	2.6	3.3	4	4.1	4.7
	Solids (g)	0	0.2	3.6	4.6	11.2	15.1
	Catalyst (g)	16.1	16.3	17.2	16.5	21	22
	Experimental loss (wt%)	2.7	2.0	1.3	2.4	11.7	1.8
	H_2 consumption/introduced	0.12	0.11	0.13	0.15	0.12	0.34
	H_2 consumption / introduced reactant (mol/mol)	0.17	0.14	0.16	0.18	0.14	0.26

Table S2 : Experimental balances of Mixture A hydroconversion as function of time (250 °C)

Figure S7 reports the gas production arising from Mixture A hydroconversion as a function of time.

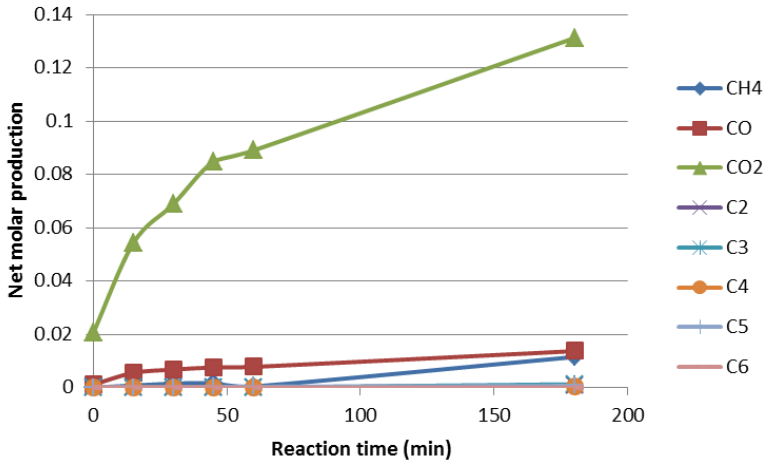

Figure S7 : Net molar production from mixture A catalytic hydroconversion (250°C)

The evolution of the main chemical functions and reactions observed for the products of catalytic hydroconversion of mixture A, according to the residence time, are reported in Figure S8.

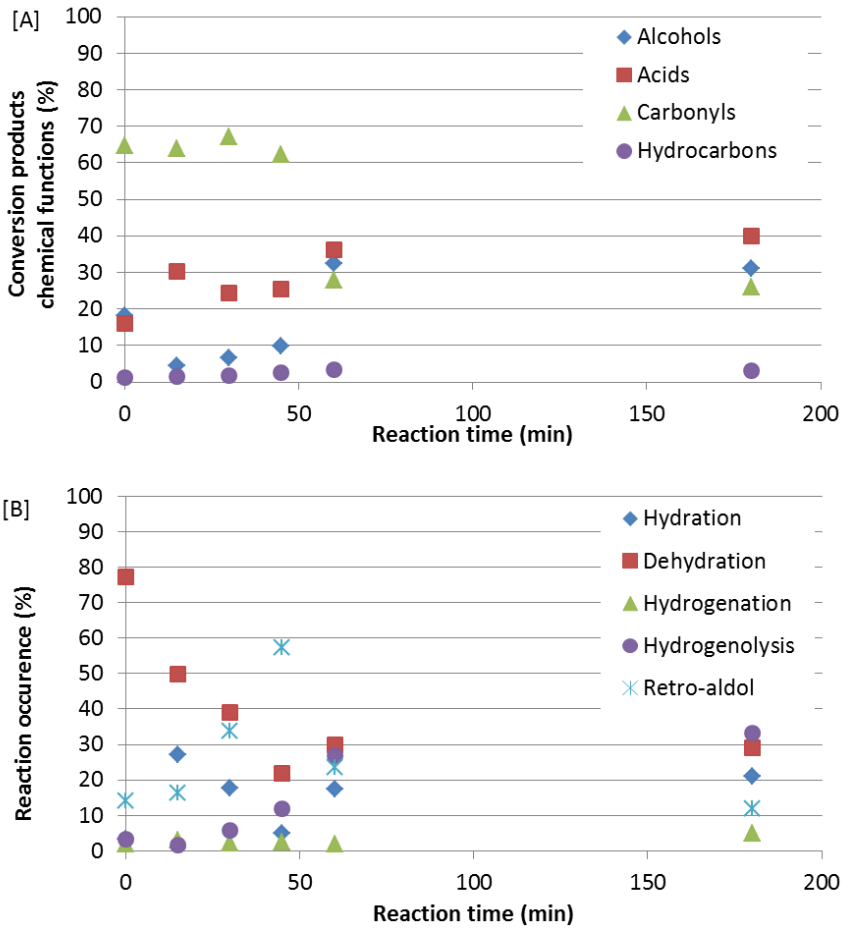

Figure S8 : Mixture A from quantified products as a function of time (250 °C) [A] Chemical functions distribution, [B] Chemical reactions distribution

It can be noted that at the early stages of the reaction, dehydration is the predominant reaction. Those reactions were likely arising from D-glucose conversion [22] even during the heating time (t0). During this period, carbonyls (including furanic species) and carboxylic acids (such as levulinic acid or lactic acid) were widely produced. As illustrated in Figure S8 [B], retro-aldol reactions and hydrogenolysis reactions leading to shorter deoxygenated molecules species only appears predominantly from 45 min. This suggests some reaction pathways modifications confirmed by Figure S8 [A] between 45 min and 60 min. Thus, GC analyzed compounds in the liquid phases were mainly composed by carbonyls and acids progressively converted into alcohols and hydrocarbons. This evolution is consistent with the H_2 consumption and appeared to arise between 45 and 60 min of reaction (see Table S2).

Figure S9 reports the normalized SEC-UV254 nm analyses of liquid phases from Mixture A as a function of time.

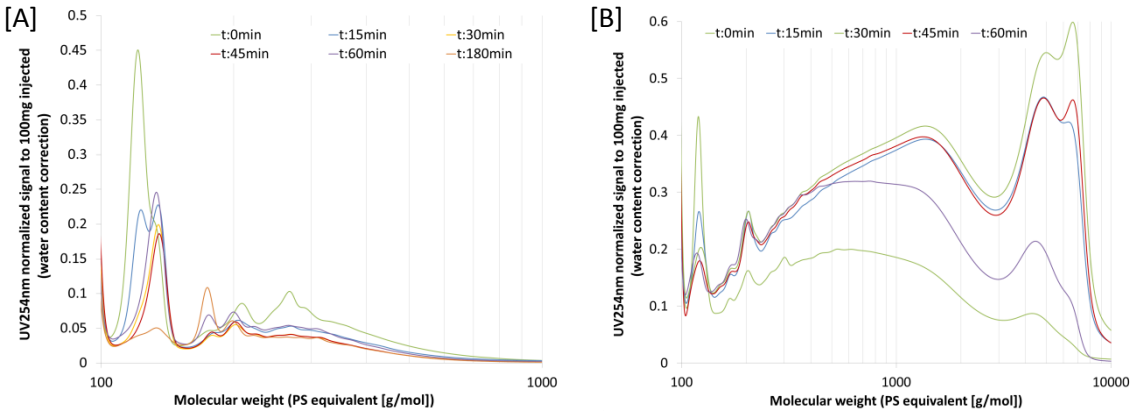

Figure S9 : Normalized SEC-UV254 nm analyses of Mixture A hydroconversion as a function of time: [A] Aqueous and [B] Organic phases (250°C)

Solid from mixtures A and B were analyzed by ^{13}C NMR. Distribution are reported in Figure S10.

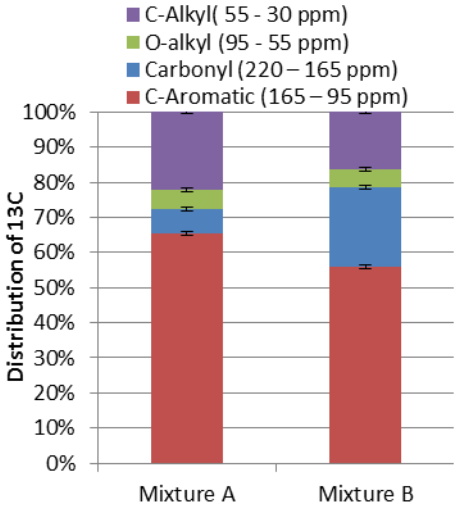

Figure S10 : ^{13}C NMR of Mixture A and B catalytic hydroconversion solid residues (250°C, 1 h)

3.3. Effect of temperature on the mixture A catalytic hydroconversion

Table S3 reports the mass balances.

Reaction temperature (°C)		**200°C**	**250°C**	**300°C**
Inlet	Liquid phase (g)	150.0	150.0	150.0
	Reduced catalyst (g)	14.3	14.3	14.4
	Introduced H_2 (g)	3.5	2.2	1.4
Outlet	Global liquid phases (g)	143.4	108.8	124.4
	• Liquid aqueous phase (g)	58.1	38.3	49.1
	• Liquid organic phase (g)	59.0	4.0	15.3
	• Washed liquid phase (g)	26.3	66.5	60.0
	Gaseous phase without H_2 (g)	1.4	4.1	6.5
	Solids (g)	0.2	11.2	3.8
	Catalyst (g)	15.6	21.0	20.6
	Experimental loss (wt%)	2.7	11.7	5.8
	H_2 consumption/introduced (mol/mol)	0.3	0.1	0.3
	H_2 consumption / introduced reactant (mol/mol)	0.5	0.1	0.3

Table S3 : Experimental balances of Mixture A hydroconversion as function of reaction temperature (1 h)

Figure S11 reports the gas production arising from Mixture A hydroconversion as a function of the temperature.

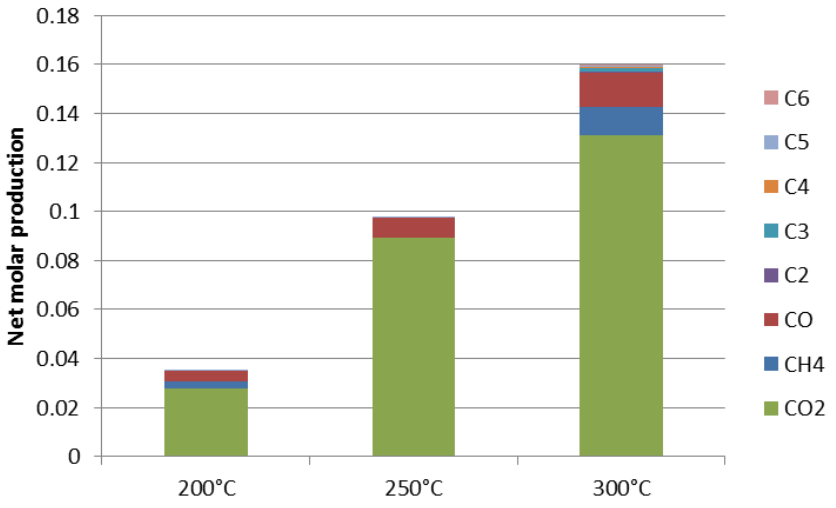

Figure S11: Net molar production from mixture A catalytic hydroconversion (1 h)

Liquid phases were analyzed by GC-FID and HPLC. Figure S12 reports the Chemical functions distribution and the chemical reaction distribution. We can observe that higher temperature led to an increase of the alcohols function production mostly from hydrogenolysis occurred.

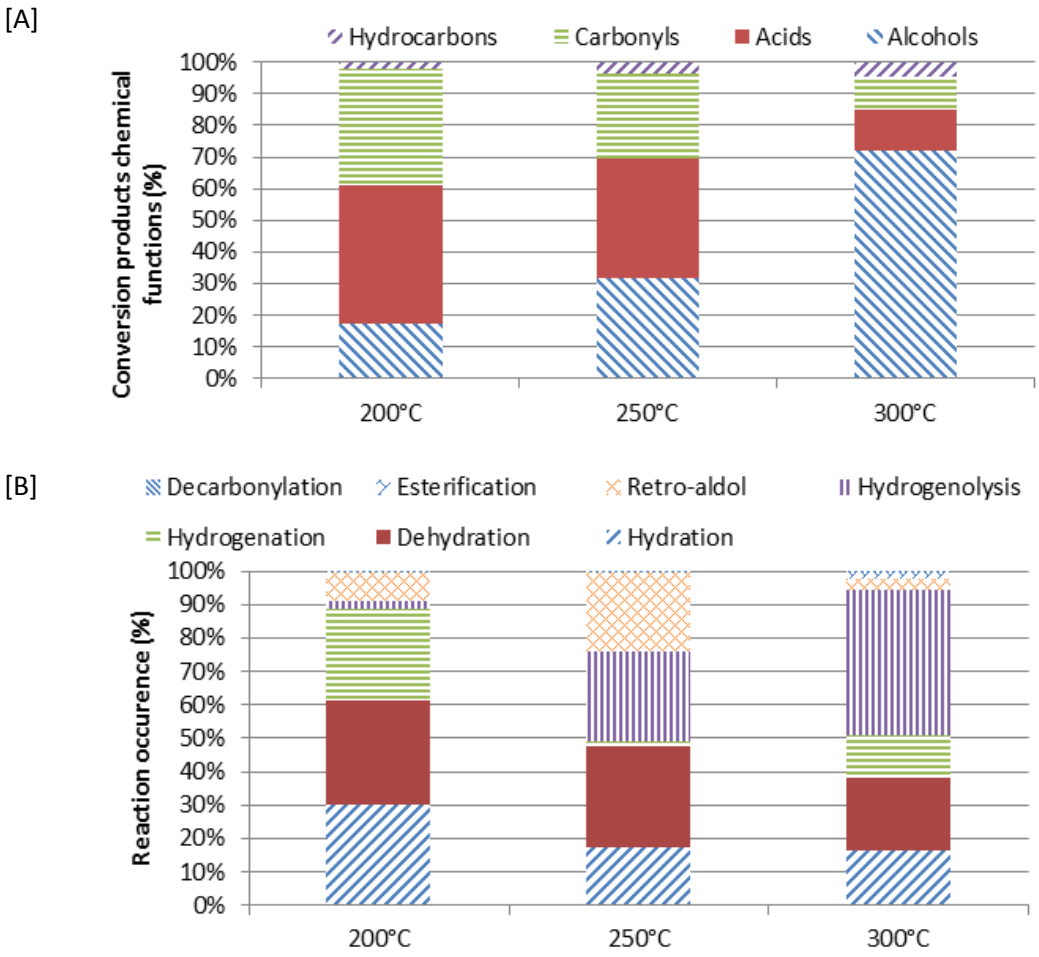

Figure S12: Mixture A quantified products as a function of the temperature (1 h) [A] Chemical functions distribution, [B] Chemical reaction distribution

Figure S13 reports the normalized SEC-UV254 nm analyses of liquid phases from Mixture A as a function of the temperature.

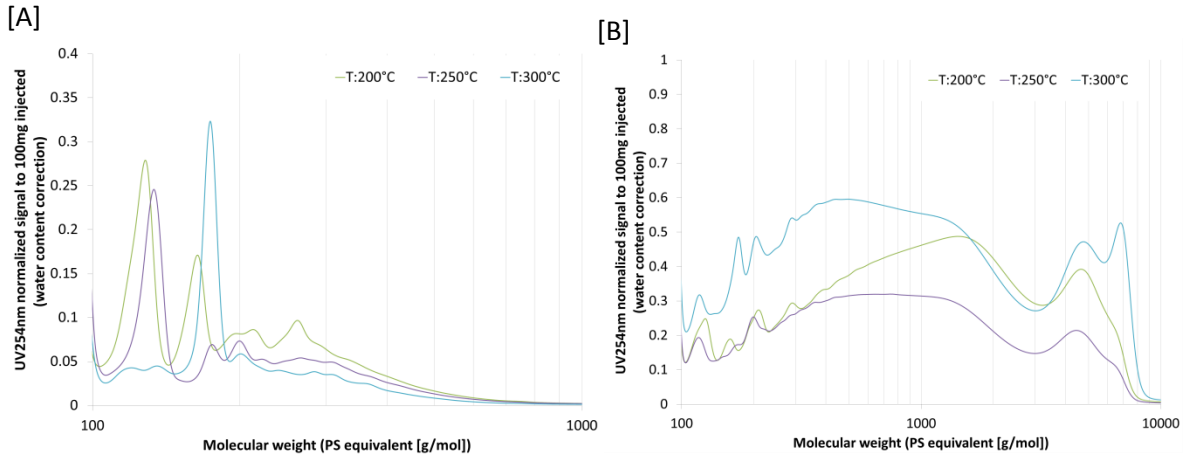

Figure S13 : Normalized SEC-UV254nm analysis of catalytic hydroconverted mixture A as function of reaction temperature (1 h) : [A] Aqueous and [B] Organic phases

Solid from mixtures A hydroconversion at 250 and 300°C were analyzed by ^{13}C NMR. Distribution are reported in Figure S14.

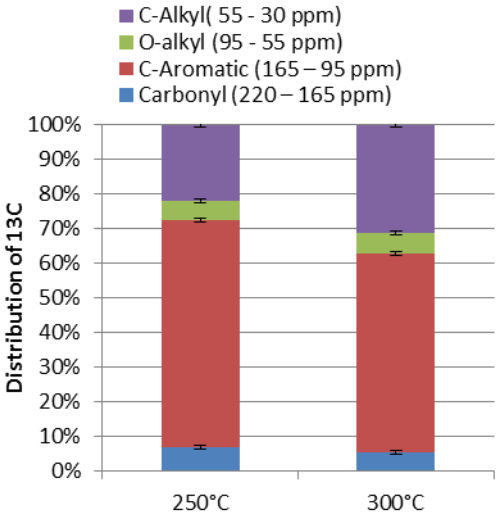

Figure S14 : ^{13}C NMR of Mixture A catalytic hydroconversion solid residues as a function of temperature (1 h)

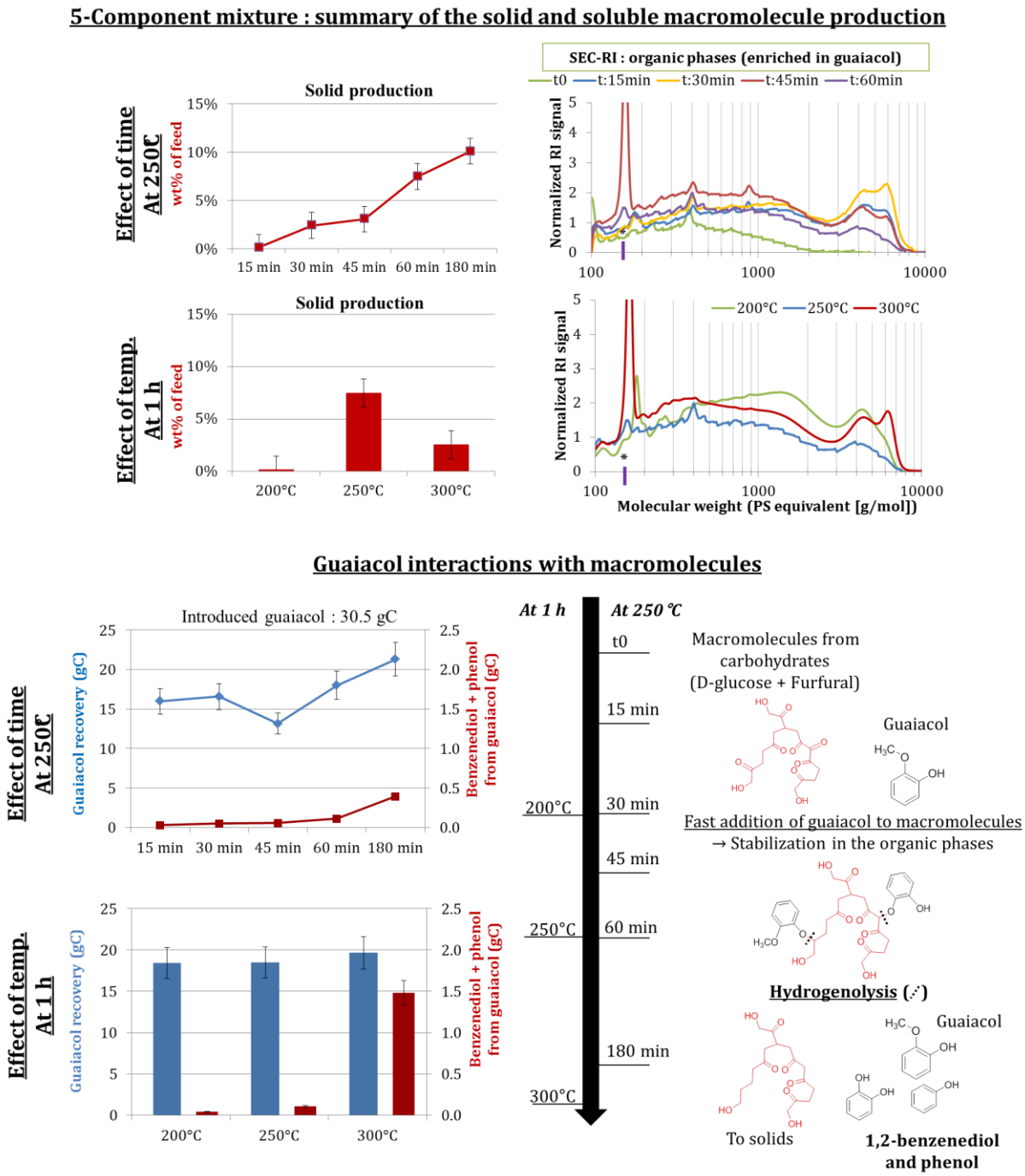

Figure S15 : Summary of the catalytic hydroconversion of the 5-component mixture depending on the reaction time and temperature